Reviews of Geophysics

REVIEW ARTICLE
10.1029/2023RG000817

Global Land Subsidence: Impact of Climate Extremes and Human Activities

Laurie S. Huning[1,2], Charlotte A. Love[2], Hassan Anjileli[3], Farshid Vahedifard[4,5], Yunxia Zhao[2], Pedro L. B. Chaffe[6], Kevin Cooper[1], Aneseh Alborzi[1], Edward Pleitez[1], Alexandre Martinez[7], Samaneh Ashraf[8], Iman Mallakpour[2], Hamed Moftakhari[9], and Amir AghaKouchak[2,5,10]

[1]Department of Civil Engineering and Construction Engineering Management, California State University, Long Beach, CA, USA, [2]Department of Civil and Environmental Engineering, University of California, Irvine, Irvine, CA, USA, [3]City of San Diego, San Diego, CA, USA, [4]Department of Civil and Environmental Engineering, Tufts University, Medford, MA, USA, [5]United Nations University Institute for Water, Environment and Health (UNU-INWEAH), Richmond Hill, ON, Canada, [6]Department of Sanitary and Environmental Engineering, Federal University of Santa Catarina, Florianópolis, Brazil, [7]Risk Management Solutions, Newark, CA, USA, [8]University of Montreal, Montreal, QC, Canada, [9]Department of Civil, Construction, and Environmental Engineering, The University of Alabama, Tuscaloosa, AL, USA, [10]Department of Earth System Science, University of California, Irvine, Irvine, CA, USA

Key Points:

- Human activities led to the largest land subsidence (LS) rates and greater human exposure to anthropogenic LS is expected in the future
- Modeling the interplay of extreme events and LS is vital as feedbacks can amplify impacts on infrastructure, the environment, and society
- Processes such as permafrost thaw and soil organic matter oxidation drive LS and release greenhouse gases, enhancing climate change

Supporting Information:

Supporting Information may be found in the online version of this article.

Correspondence to:

L. S. Huning,
laurie.huning@csulb.edu

Citation:

Huning, L. S., Love, C. A., Anjileli, H., Vahedifard, F., Zhao, Y., Chaffe, P. L. B., et al. (2024). Global land subsidence: Impact of climate extremes and human activities. *Reviews of Geophysics*, *62*, e2023RG000817. https://doi.org/10.1029/2023RG000817

Received 27 MAY 2023
Accepted 4 SEP 2024

Abstract Globally, land subsidence (LS) often adversely impacts infrastructure, humans, and the environment. As climate change intensifies the terrestrial hydrologic cycle and severity of climate extremes, the interplay among extremes (e.g., floods, droughts, wildfires, etc.), subsidence, and their effects must be better understood since LS can alter the impacts of extreme events, and extreme events can drive LS. Furthermore, several processes causing subsidence (e.g., ice-rich permafrost degradation, oxidation of organic matter) have been shown to also release greenhouse gases, accelerating climate change. Our review aims to synthesize these complex relationships, including human activities contributing to LS, and to identify the causes and rates of subsidence across diverse landscapes. We primarily focus on the era of synthetic aperture radar (SAR), which has significantly contributed to advancements in our understanding of ground deformations around the world. Ultimately, we identify gaps and opportunities to aid LS monitoring, mitigation, and adaptation strategies and guide interdisciplinary efforts to further our process-based understanding of subsidence and associated climate feedbacks. We highlight the need to incorporate the interplay of extreme events, LS, and human activities into models, risk and vulnerability assessments, and management practices to develop improved mitigation and adaptation strategies as the global climate warms. Without consideration of such interplay and/or feedback loops, we may underestimate the enhancement of climate change and acceleration of LS across many regions, leaving communities unprepared for their ramifications. Proactive and interdisciplinary efforts should be leveraged to develop strategies and policies that mitigate or reverse anthropogenic LS and climate change impacts.

Plain Language Summary Our article reviews existing research on the global issue of land subsidence (LS), or the relative sinking of the land surface. At the global scale, a variety of LS drivers and physical processes are present and interact with one another. The combination of climatic extremes (e.g., droughts, floods, wildfires, etc.) and LS can lead to devastating impacts on natural and built systems as well as feedbacks within our Earth system that enhance climate change. Yet, a review of the combined effects of extreme events, climate, subsidence, and their impacts, does not currently exist. In this article, we identify and characterize LS drivers, rates, and impacts throughout many different climates (e.g., arid and humid regions) and landscapes (coastal and inland locales, urban and agricultural areas). We also bring together the interplay among extreme events and LS and their connections to climate, human activities, and infrastructure. Integrating such relationships into LS analysis and monitoring frameworks is necessary to better understand cascading hazards and identify vulnerable populations, assess at-risk infrastructure, and develop mitigation and adaptation strategies for LS.

1. Introduction

Land subsidence (LS) is a pressing global issue warranting immediate and continued attention. Subsidence, the relative lowering or sinking of the land surface, causes significant infrastructure damage, environmental

problems, and societal impacts, totaling billions of dollars in economic losses annually (R. L. Hu et al., 2004; Oppenheimer et al., 2019). Natural and anthropogenic factors (e.g., compaction, natural resources exploitation, permafrost degradation, peatland burning, dewatering, urbanization) combine to form a complex pattern of LS rates and impacts stretching from coastal to inland areas worldwide. By unraveling the intricate responses of the land surface to different drivers and characterizing their contributions to subsidence, especially related to the climate system, we will be able to develop better mitigation and adaptation strategies and understand subsidence effects across different regions. While the ramifications of climatic extreme events and LS affect one another, additional research is still needed in this area.

As the global climate warms and amplifies the terrestrial hydrologic cycle (AghaKouchak et al., 2020; IPCC, 2021), extreme climatic events and LS impacts will increasingly affect one another across many parts of the world (IPCC, 2021; Melvin et al., 2017). Such relationships are already evident. High levels of LS were observed where the devastating levee failures occurred in New Orleans (USA) during Hurricane Katrina in 2005 (Dixon et al., 2006; NOAA, 2018). In 2017, regions of Houston (USA) with the largest LS also experienced the most severe flooding from Hurricane Harvey (Miller & Shirzaei, 2019), which contributed to at least 65 deaths from drowning, over 200,000 flood-damaged buildings, and at least $125 billion in total damages (NOAA, 2018). When combined with subsidence, the compounding effects of expanding megacities and coastal communities, sea level rise, and extreme precipitation exacerbate the exposure and vulnerability of an increasing population to flooding (Cao et al., 2021; Nicholls et al., 2021; Oppenheimer et al., 2019; Tessler et al., 2015; Wahl et al., 2015). Other climate-driven extremes (e.g., wildfires, drought) heighten the risk of LS or intensify this hazard. For example, as temperatures warm and Arctic wildfires spread, thawing ice-rich permafrost places critical infrastructure (e.g., pipelines) at-risk as the land subsides with the loss of the frozen soil's structure (Gibson et al., 2018; Holloway et al., 2020; Karjalainen et al., 2020). The effects of subsidence can alter the potential impacts of extreme events, and extreme events can contribute to LS. Furthermore, some processes that facilitate subsidence (e.g., permafrost degradation and soil organic matter oxidation), also present significant positive climate feedbacks that enhance climate change when trapped greenhouse gases from the soil escape to the atmosphere (Gibson et al., 2018).

Despite the devastating impacts that the combination of climatic extremes and subsidence have on natural and built systems, a review of the interplay among extreme events, climate, subsidence, human activities, and their impacts, remains a critical gap in understanding cascading hazards and complex feedbacks. An improved understanding of the feedback loops between these processes is necessary for identifying vulnerable populations, at-risk infrastructure, and also future research directions to address current gaps in this area, and developing suitable mitigation and adaptation strategies. Recent satellite-era technologies have made such investigations possible. Yet, existing reviews commonly examine subsidence in only certain regions (e.g., coastal areas (Shirzaei et al., 2021)) or from specific causes (e.g., groundwater-driven (Herrera-García et al., 2021)) with few studies classifying the diverse factors causing subsidence across the globe (Bagheri-Gavkosh et al., 2021). Nevertheless, existing reviews do not examine the important interplay and feedback between extreme events and LS and their connections to climate and infrastructure. By reviewing recent literature, we provide a global survey of LS rates and causes across manifold landscapes and climate regions (e.g., coastal and inland areas, cities and agricultural centers, and arid and humid regions). We also synthesize process-based combined effects among climatic extremes, subsidence, human activities, and their impacts, by discussing a variety of observed examples and projections around the world. Finally, we identify existing knowledge gaps and opportunities that will help guide the global monitoring and mitigation of subsidence impacts within our complex climate system.

2. Monitoring and Modeling Land Subsidence

LS can occur gradually (e.g., fluid extraction) or rapidly (e.g., earthquake activity, mining collapse) and over localized (order of a few to tens of square meters; e.g., sinkhole from limestone dissolution) or large regions (order of one to tens of square kilometers or more, e.g., California's Central Valley (USA), Bangkok (Thailand), the Guangdong–Hong Kong–Macao Greater Bay Area (China), Jakarta (Indonesia), Gippsland Basin (Australia), Ravenna (Italy)) with measurable downward displacements of the Earth's surface (M. Ao et al., 2015; Cao et al., 2021; Faunt et al., 2016; Jago-on et al., 2009; Marker, 2013; Ng et al., 2015; Teatini et al., 2005). A variety of technologies are used to monitor LS (e.g., leveling, inclinometers, tiltmeters, borehole extensometers, observation wells, Global Positioning Systems (GPS), and Synthetic Aperture Radar (SAR)) (Ferretti et al., 2015; Galloway & Hoffmann, 2007; Motagh et al., 2008; Wang & Soler, 2015). Herein, we do not aim to review sensor

technologies, monitoring techniques, or data processing methods as several comprehensive studies in these areas exist (Bürgmann et al., 2000; Cruz et al., 2022; Musa et al., 2015; Ouchi, 2013; Rosen et al., 2000; Wang & Soler, 2015). Instead, we focus on global LS rates, their drivers, and potential impacts. Nonetheless, we briefly discuss SAR and the Interferometric SAR (InSAR) approach since we collected data from literature using satellite-based SAR observations to provide a consistent framework for comparing subsidence rates in Figures 1 and 2 (discussed below). Further, several studies have leveraged numerical modeling alone or in combination with monitoring techniques, such as InSAR, to simulate subsidence processes and assess hydromechanical behavior of aquifers/aquitards (e.g., Bockstiegel et al., 2023; Bonì et al., 2020; Calderhead et al., 2011; Catalao et al., 2016; Galloway & Burbey, 2011; Zhang & Burbey, 2016). Numerical modeling is undoubtedly a valuable tool for studying LS, as evidenced by its widespread use in the literature. However, the primary focus of this review article is to critically synthesize the literature on the interplay of climatic extremes and LS. The emphasis is placed on discussing the underlying factors and processes that contribute to the dynamics of climatic extremes and LS. While we certainly acknowledge the relevance of previous studies employing various modeling tools (e.g., numerical modeling) and monitoring techniques (e.g., InSAR), it is essential to clarify that a comprehensive review of the existing methods for numerical modeling and monitoring of LS falls beyond the scope of this article.

2.1. Satellite-Based SAR Observations and InSAR

Advances in satellite remote sensing with SAR have moved us closer to monitoring and mapping LS and monitoring its rates globally (e.g., Davydzenka et al., 2024). Since SAR-based information is used to infer ground deformation on the order of several millimeters per year (Bürgmann et al., 2000; Ferretti et al., 2007; Ouchi, 2013; Zhou et al., 2009), it often aids impact assessment across a variety of fields (e.g., agriculture, infrastructure monitoring, land management, geology, seismology, hydrology) (Baghdadi et al., 2007; Bru et al., 2013; Brunori et al., 2015; Ferretti et al., 2015; Forkuor et al., 2014; Musa et al., 2015; Ouchi, 2013; Rosen et al., 2000).

In fact, the InSAR technique was developed to leverage the wavelength phase and amplitude information in SAR imagery. InSAR derives an interferogram by computing the phase difference between two SAR snapshots over an area, which is used to track surface deformation (Klein et al., 2017; Miller & Shirzaei, 2015; Sánchez-Gámez & Navarro, 2017). Traditional InSAR techniques provide deformation estimates along the line-of-sight direction of the sensor relative to the position of the satellite during orbit (e.g., ascending or descending) (Du et al., 2023; Erten et al., 2010; Motagh et al., 2008). Multiple methods exist for processing the phase information (e.g., Differential InSAR [DInSAR], Permanent Scatterers InSAR [PSInSAR]) (Ferretti et al., 2001; Ouchi, 2013; Peltier et al., 2010).

SAR satellites often carry a single wavelength sensor (i.e., L-band [23.5 cm wavelength], C-band [5.6 cm], X-band [3.1 cm]), but multi-frequency sensors also exist (Ouchi, 2013; Shirzaei et al., 2021). Depending on the radar wavelength, the spatial resolution of SAR is on the order of meters to tens of meters (Merryman Boncori, 2019). Shorter wavelengths yield higher spatial resolutions. Given that radar wavelength is related to the spatial resolution of imagery, how the signal interacts with a surface, and the distance the signal penetrates into a medium, SAR-based information lends itself to a variety of applications (Tsokas et al., 2022). For example, X-band sensors are mainly used for collecting urban observations with built infrastructure since shrubs and canopies highly scatter the short wavelengths (Castellazzi et al., 2016; Tsokas et al., 2022), whereas L-band SAR penetrates dense vegetation and shows greater coherence than data from C- and X-bands (Kasischke et al., 2007; Ottinger & Kuenzer, 2020; Raucoules et al., 2007; Shirzaei et al., 2021; Tsokas et al., 2022; Tsyganskaya et al., 2018). When SAR-based information is combined with auxiliary data (e.g., groundwater pumping rates, geology, shear wave velocity), an improved understanding of the causes of observed subsidence and their potential impacts is achievable (Fielding et al., 1998).

SAR sensors use active remote sensing by emitting electromagnetic radiation in the microwave spectrum, allowing them to operate during both day and night and penetrate cloud cover with their longer wavelengths (Ottinger & Kuenzer, 2020; Raucoules et al., 2007). Nonetheless, meteorological conditions can cause atmospheric artifacts, and if not correctly identified or considered, they could lead to misinterpretations of ground deformations. Furthermore, careful selection of interferometric pairs is important for minimizing the loss of coherence, which is affected by factors such as changing land cover conditions (e.g., agricultural areas), the temporal lag between images, and applications. Single-sensor SAR images tend to have low resolution or small

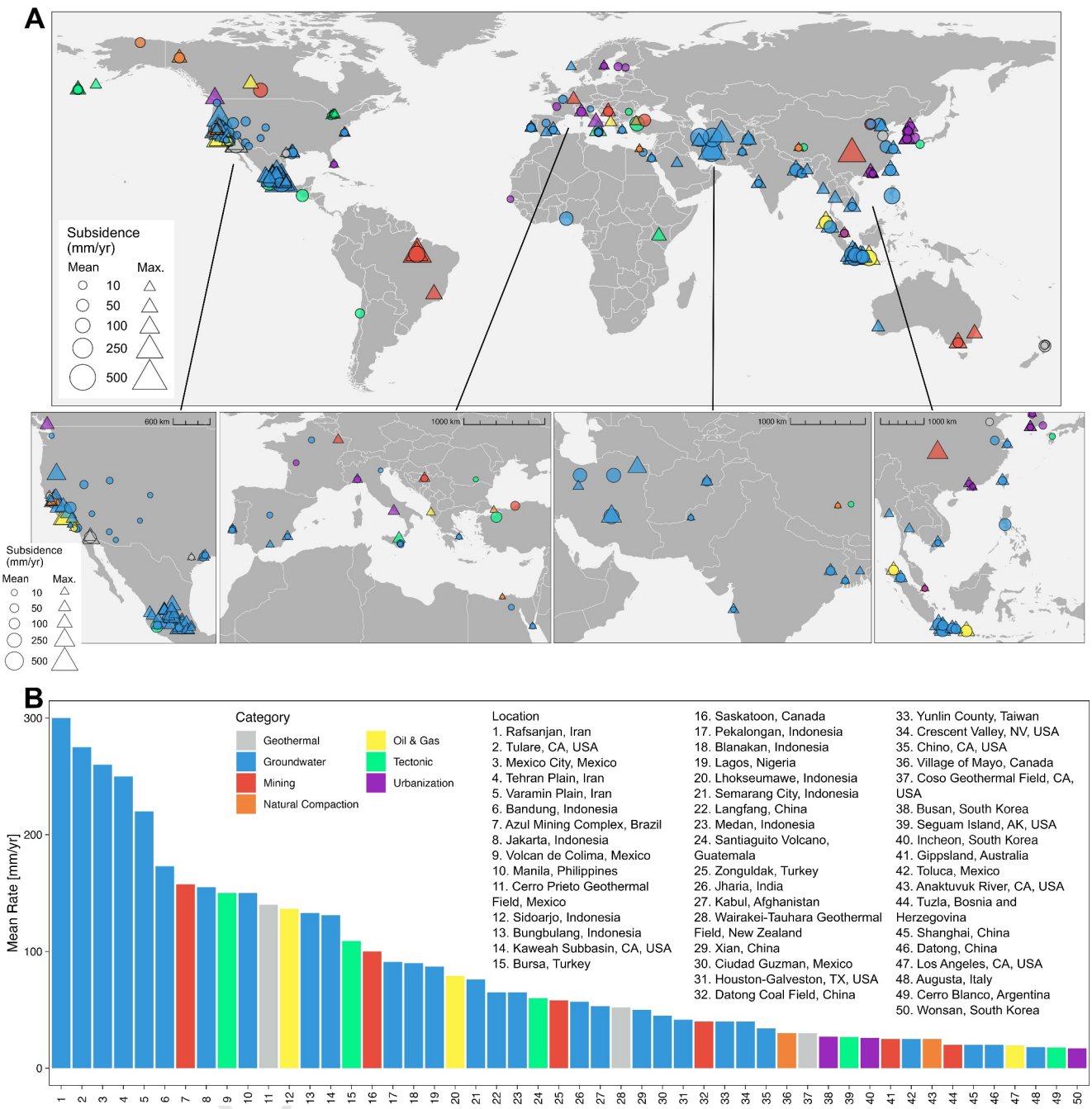

Figure 1. Reported land subsidence rates and drivers across the globe. (a) Global map of main LS drivers (colors) with mean (circles) and maximum (triangles) rates (shape sizes). For the regional maps, shape sizes are defined in the leftmost panel. We use a shared color scheme (legend shown in (b)) to represent the primary causes of subsidence in both (a) and (b). (b) Global comparison of the 50 largest mean subsidence rates. Indices along the x-axis correspond to the listed locations. (This figure is based on our assessment of literature (Text S1 in Supporting Information S1) and information therein. The subsidence rates reported here were taken from literature and calculated as described therein. Note that LS rates change over time, occur at a variety of time scales, and exhibit nonlinear variability. Also, given the range of different locations and studies assessed, not all rates were observed over the same time period or estimated similarly. LS rates of approximately 300 mm/yr for the Rafsanjan Plain in Iran have been reported as both the maximum (Motagh et al., 2017) and mean (Bagheri et al., 2019) values. Meldebekova et al. (2020) reported the same value for the mean and maximum rates in Kabul, Afghanistan).

coverage in comparison to multi-sensor SAR investigations for LS applications (Raspini et al., 2022). As noted above, since entire reviews exist that focus on SAR-based applications for LS monitoring (e.g., Raspini et al., 2022; Raucoules et al., 2007), we only briefly summarize a few key advantages and limitations herein.

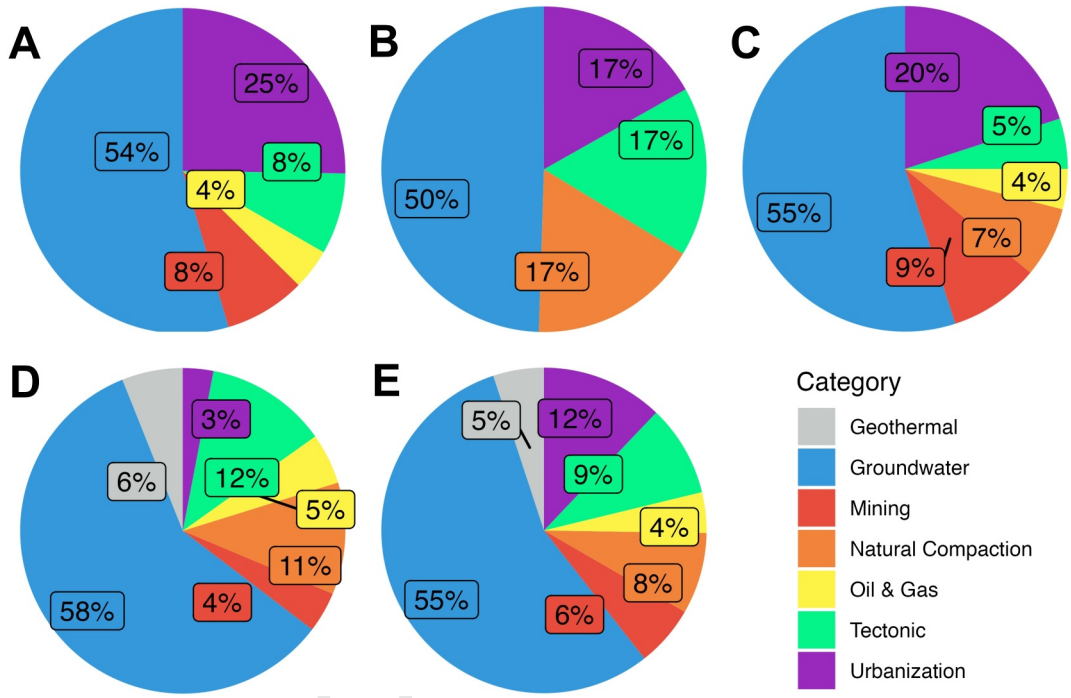

Figure 2. Distribution of literature reviewed in this study by LS driver in the following regions: (a) Europe, (b) Africa, (c) Asia and Oceania, (d) North and South America, and (e) all global sites from Figure 1. (This figure is based on our assessment of literature (Text S1 in Supporting Information S1) and information therein. It does not account for all possible drivers or subsidence cases across a region, nor does it include an area or weighted average. Rather it is a summary of the literature reviewed in this study and attribution of LS to a single driver is a challenging process).

3. Natural and Anthropogenic Land Subsidence

Natural processes and human activities drive LS globally (Bagheri-Gavkosh et al., 2021; Marker, 2013). Some driving processes naturally occur and are also influenced by anthropogenic activities. Permafrost degradation serves as one example driver that naturally occurs with seasonal temperature fluctuations, but is also driven or amplified by urbanization and anthropogenic climate change (e.g., warming temperatures and climate change-driven wildfires and heatwaves) (Streletskiy et al., 2015). We classify subsidence into two broad categories, natural and anthropogenic, based on its primary identified cause. Naturally occurring processes including seasonal or inter-annual variations in groundwater levels, volcanic activity, tectonic deformation, soil/rock dissolution, natural consolidation, and the decomposition of organic materials drive natural LS. Whereas human-related activities, such as the withdrawal of natural resources (e.g., fossil fuels, groundwater, geothermal fluids), cultivation or burning of peatlands, wetland removal, and the loading of rapid urban development, propel anthropogenic LS.

Anthropogenic influences are widely documented as the dominant driving force (by orders of magnitude) over natural subsidence processes across many regions (Chaussard et al., 2013; Gambolati et al., 2005; Kondolf et al., 2022; Syvitski et al., 2009). Human activities often exacerbate a natural subsidence rate as evidenced by the rapid urbanization and groundwater extraction that contributed to Otura, Spain subsiding at a rate of 10 mm/yr, while tectonics throughout the region only accounted for a maximum of 1 mm/yr (Sousa et al., 2010). Other prime examples where anthropogenic subsidence exceeds natural subsidence rates include: Iran (Rafsanjan, Tehran), USA (Wilmington, California; Charleston, South Carolina; Houston-Galveston area in Texas; California's Central Valley), Italy (Po Plain), and Egypt (Cairo), China (Beijing), Mexico (Mexico City), and India (New Delhi) (Aly et al., 2009; ASCE Land Subsidence Task Committee, 2022; Bagheri et al., 2019; Carminati & Martinelli, 2002; Cigna & Tapete, 2021; Famiglietti, 2014; Gambolati et al., 2005; Garg et al., 2022; Y. Liu et al., 2020; Mahmoudpour et al., 2013; Motagh et al., 2017; Richey et al., 2015; Zhu et al., 2015). Although multiple factors may drive subsidence at a given location, we focus on the identified dominant factors based on and synthesized from literature (Figures 1 and 2). We note that LS in many parts of the world is not well-studied,

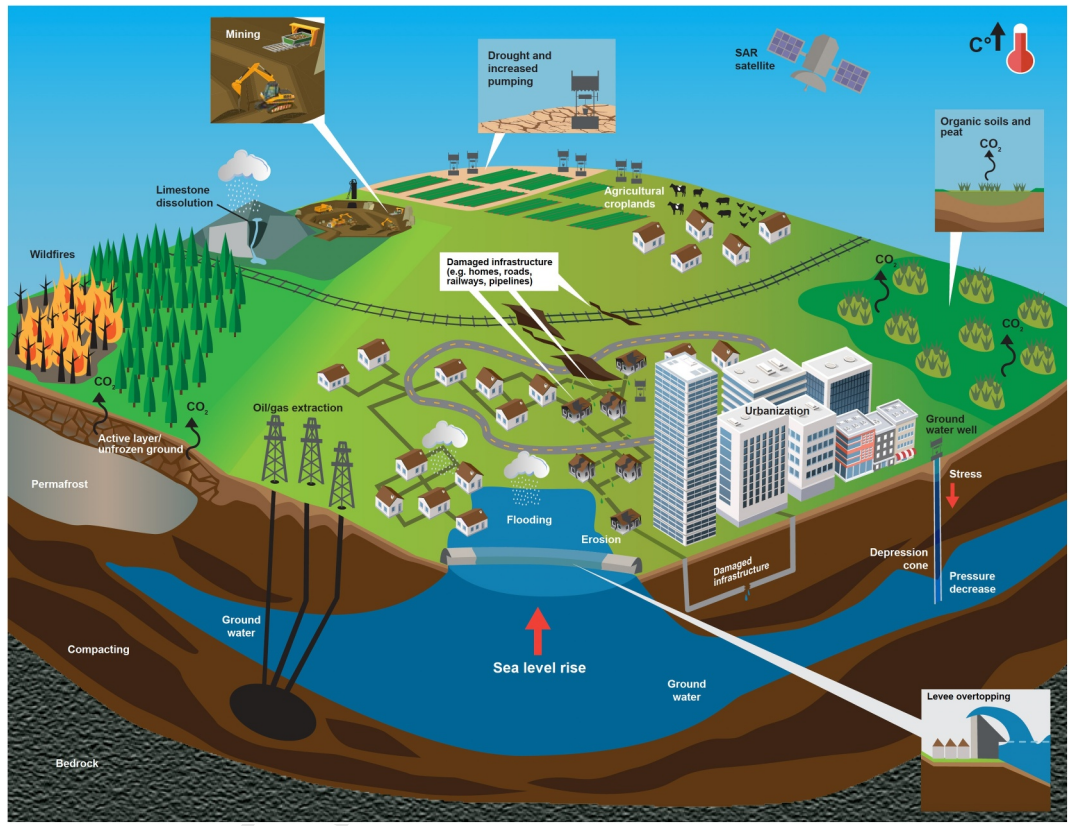

Figure 3. Land subsidence and climate extreme interplay and combined effects of human activities.

measurement uncertainties exist, and attributing the individual contribution of a driver to land deformation is often difficult. Furthermore, we provide a survey of literature, which should not be considered a comprehensive examination of all published LS studies.

4. Global Survey of Land Subsidence Causes and Hotspots

Using SAR-based studies, we survey subsidence rates and causes for nearly 200 unique locations across the world (Figure 1). It should be noted that LS has a different temporal structure depending on the geology of the region and the LS driver. Furthermore, LS rates vary in both space and time, and therefore, cannot be assumed to be ongoing or constant. Given this and the nonlinearity of LS rates, current rates should not be taken to imply future LS rates. Here, we describe several of these processes contributing to the complex subsidence patterns observed (Figure 3).

4.1. Natural Resource Extraction

For centuries, agriculture and the extraction of natural resources (e.g., groundwater, oil, and gas) from the Earth have shaped landscapes. Groundwater withdrawals have become more prevalent with increasing climate variability, agricultural irrigation, and population demands (Arnell, 2004; Awasthi et al., 2022; Erkens et al., 2016; IPCC, 2021; Wada & Bierkens, 2014; Wada et al., 2011). Land deformations caused by groundwater fluxes manifest in two primary ways: elastic and inelastic. Elastic deformation can occur due to natural seasonal variations in water levels or even long-term deformation, if the pre-consolidation pressure (i.e., the maximum historical pressure the soil has experienced) is not exceeded. Hence, seasonal deformation is elastic, but long-term deformation can also be recoverable (Ezquerro et al., 2014). On the other hand, inelastic deformation may occur due to significant overdraft. Groundwater extraction often leads to sediment compaction and unrecoverable, permanent loss of aquifer storage capacity (Awasthi et al., 2022; Miller et al., 2020). Increased effective stress through loss of pore-water pressure and reduced pore volume causes irreversible compaction of low permeability layers (Miller et al., 2017). Therefore, collecting observations at a given site over consecutive full year periods,

rather than a single season (e.g., summer) even if observed annually, provides a more robust understanding of LS rates as they vary in time and have seasonal influences as well as a better indication of whether deformation is controlled by elastic or inelastic compaction (Motagh et al., 2008).

Groundwater extraction is the primary (human-induced) factor causing subsidence (Bagheri-Gavkosh et al., 2021), accounting for subsidence at approximately 55% of the global sites we surveyed (Figure 2e). The greatest number of these sites occur in North America and Asia. The largest mean subsidence rate reported and driven by groundwater extraction is approximately 300 mm/yr in the Rafsanjan Plain region in Iran (Figure 1b), which is well-known for pistachio production (Bagheri et al., 2019). A maximum subsidence rate of 300 mm/yr localized near Rafsanjan, Iran was also attributed to groundwater extraction, with rates >50 mm/yr over the 1,000 km^2 surrounding Koshkoueieh-Rafsanjan region (Motagh et al., 2017). Other cities and regions with large (>200 mm/yr) average subsidence rates due to groundwater extraction include the San Joaquin Valley (275 mm/yr), Mexico City (260 mm/yr), Tehran (250 mm/yr), and Varamin (220 mm/yr) (Chaussard et al., 2021; Haghshenas Haghighi & Motagh, 2019; Khorrami et al., 2023; Ojha et al., 2020). To minimize the loss of aquifer capacity and subsidence, some areas (e.g., USA [Las Vegas; Kansas], China [Taiyuan basin]) recharge their groundwater systems to prevent damage from overdraft, recover elevation declines, and develop sustainable management policies (e.g., California's Sustainable Groundwater Management Act [SGMA]) (Neely et al., 2021; Ojha et al., 2020; Sophocleous, 2005; Tang et al., 2022).

Oil and gas extraction from underground formations has contributed to an estimated 4% of global LS sites surveyed, as shown in Figure 2e. Typically, these processes facilitate more localized subsidence than groundwater pumping (Gambolati et al., 2005). When these resources are extracted, reduced pore pressure within the reservoir leads to compaction under the overlying materials' weight (Gurevich & Chilingarian, 1993). An area of subsidence over 12,000 km^2 in the coastal San Jacinto region of Texas, for instance, is affected by fluid pumping, primarily from groundwater withdrawals (Gabrysch & Neighbors, 2005), and to a lesser extent from oil and gas extraction (Holzer & Bluntzer, 1984). In the absence of groundwater abstraction, the oil fields of Lost Hills, California have experienced maximum subsidence rates reported in excess of 400 mm/yr (Fielding et al., 1998). Several areas across the Gulf Coast of the U.S. have seen LS rates exceeding 10 mm/yr, with oil and gas extraction contributing to the maximum observed rate in the region of 56 mm/yr at the Stratton Ridge Oil Field, Texas (Qu et al., 2023). Observations in the Cold Lake heavy oil field (Alberta, Canada) exhibit substantial vertical deformation exceeding 36 cm in a month from producing bitumen, but did not indicate permanent subsidence since cyclic steam stimulation (injection, soaking, and pumping) helps recover the land elevation (Stancliff & van der Kooij, 2001).

Demand for natural resources soars with socioeconomic expansion and urbanization (Awasthi et al., 2022; Dang et al., 2014; Hayashi et al., 2009; Wada & Bierkens, 2014; Wada et al., 2011). Underground mines, prevalent in the former coal-rich regions of Europe and in current mining operations in Ukraine, Poland, and China, catalyze short- and long-term local and regional ground deformations (Peng, 2008). Methane extraction was identified as the primary factor causing the 3–5 m of LS observed during the twentieth century in the Po Delta and Plain (Giosan et al., 2014), where roughly one-third of Italy's population resides (Carminati & Martinelli, 2002; Herrera-García et al., 2021). Also, coal and iron mining operations have led to thousands of active and abandoned underground tunnels. Over 300 km of underground tunnels previously used as quarries lie under Paris, and around 1,000 km-mine galleries/km^2 lie in the coal-rich northern France (Hachez-Leroy, 2014). Activities such as mining for minerals and hydrocarbons creates voids in the subsurface, with the eventual collapse of these voids contributing to soil compaction and LS, especially in extensive mining operations. Sudden mine gallery collapses cause pit subsidence (local) and sag subsidence (larger scale), which have been found to spread over several hectares (Marino & Gamble, 1986) decades after their closure (Samsonov et al., 2013).

4.2. Urbanization

Urban developments can compact underlying soils depending on several factors such as soil type, soil loading history and mechanical properties, geological conditions, and the nature of urban development practices in a given area (F. Chen et al., 2012; Holtz & Kovacs, 1981; Nawaz et al., 2013; Tiwari et al., 2023). The construction of new buildings, roads, and other infrastructure in urban areas due to urbanization often involves significant loads being placed on the soil (Z. Ao et al., 2024). Over time, this additional load can compress the soil, leading to a reduction in pore space and increased soil density, a process known as soil compaction (Holtz & Kovacs, 1981;

Nawaz et al., 2013). The magnitude of soil compaction and the resulting soil settlements depend on the soil loading history and mechanical properties. If the additional loads from urbanization are less than the maximum historical pressure the soil has undergone, the soil will exhibit limited settlement due to the added loads. Conversely, if the added loads represent the highest load in the entire history of the soil, substantial settlement may occur due to the new loading patterns from urbanization (F. Chen et al., 2012; Holtz & Kovacs, 1981; Nawaz et al., 2013).

Further, urbanization is often associated with increased demand for water, leading to extensive and unsustainable groundwater extraction, which exacerbates groundwater level decline and elevates subsidence risk (Dong et al., 2014; Galloway & Burbey, 2011). As groundwater is pumped out, the water table drops, and the soil particles lose buoyant support, causing them to compact and leading to LS (Ezquerro et al., 2014). Beijing is an example of one city in China where both urbanization and groundwater extraction drive LS rates up to 110 mm/yr (B. Hu et al., 2014). An estimated 45% of China's major cities experience LS rates exceeding 3 mm/yr, which affects about 29% of the nation's urban population, and 16% of its cities are sinking faster than 10 mm/yr (Z. Ao et al., 2024). Urbanization alone primarily accounts for 12% of sinking global sites we surveyed (Figure 2e).

Urbanization can also accelerate natural subsidence processes (Parsons et al., 2023). In the Mississippi and Ganges-Brahmaputra-Meghna Deltas, natural subsidence is hypothesized to be underway due to factors like sediment compaction, where sediments are transported and deposited, resulting in sediment loading and isostatic adjustment, and sea level changes; however, isolating a single factor or even the contributions of one or more drivers of LS at a particular site remains challenging, especially since LS rates and drivers are time dependent (Blum et al., 2008; F. Chen et al., 2012; Grall et al., 2018; Parsons et al., 2023; Wolstencroft et al., 2014). In other coastal areas and large river deltas where natural subsidence is high, urbanization, coupled with human activities such as the extraction of hydrocarbons and/or groundwater, expedites these natural subsidence processes (e.g., Manila, Philippines; Galveston, Texas, USA; Po Delta, Italy; Chao Phraya Delta, Thailand; Rhine-Meuse Delta, the Netherlands) (Giosan et al., 2014; Oppenheimer et al., 2019; Shirzaei et al., 2021). Deltas and coastal regions also face rising sea levels that place subsiding regions at even higher flood risk (e.g., Galveston Bay contends with a relative sea level rise (SLR) rate [the combination of regional SLR and local subsidence] that is approximately four times greater than the global average (Y. Liu et al., 2020) and the maximum subsidence rates observed in coastal Tianjin, Semarang, and Jakarta are nearly 15 times more than the global mean SLR (Wu et al., 2022)). Globally (Figure 2e), and regionally for Europe (Figure 2a) and Asia-Oceania (Figure 2c), urbanization is the second largest driver of subsidence according to the literature. However, in North and South America (Figure 2d) tectonics and natural compaction are the second and third greatest drivers, respectively. In Africa (Figure 2b), these three drivers (urbanization, tectonics, and natural compaction) are identified as the primary factors leading to LS for an equal number of sites in the literature.

From our synthesis of literature for SAR-based LS rates, anthropogenic activities are the principal sources of subsidence at ~82% of the locations in Figure 1. Out of the top 50 rates, 43 have drivers that fall into this category (Figure 1b). In addition to those drivers already discussed, extreme and compound events are increasing in their frequency, severity, and intensity across much of the world (IPCC, 2021) and their impacts influence and are influenced by subsidence.

5. Extreme and Compound Events and Land Subsidence Impacts

5.1. Coastal Regions and Flooding

LS may not be the sole factor triggering catastrophic damages or failures in buildings and lifeline infrastructure systems (Shiklomanov et al., 2017) because it is commonly compounded by other climatic trends (e.g., SLR, warming temperatures) and/or extreme events (e.g., hurricane, flood, drought, earthquake). Subsidence alters flow and runoff patterns, exposing additional areas to urban flooding and nonlinearly affecting the spatial distribution of flooding (Ohenhen, Shirzaei, Ojha, et al., 2024; Yin et al., 2016). Throughout many of the world's coastal and deltaic megacities, anthropogenic LS increases the vulnerability and exposure of large populations and infrastructure to urban flooding (e.g., Jakarta, Manila, New Orleans, Tokyo) (Jago-on et al., 2009; Showstack, 2014; Syvitski et al., 2009; Tessler et al., 2015) (Figure 3). In the Chesapeake Bay region (USA), Eggleston and Pope (2013) estimated that LS accounted for about half of the relative SLR, which accelerates local sinking. More recently, heterogeneous subsidence across the Chesapeake Bay area was estimated to be up to 5.5 mm/yr (Sherpa et al., 2023). In this region and many others where subsidence is high, there is an increasing trend in

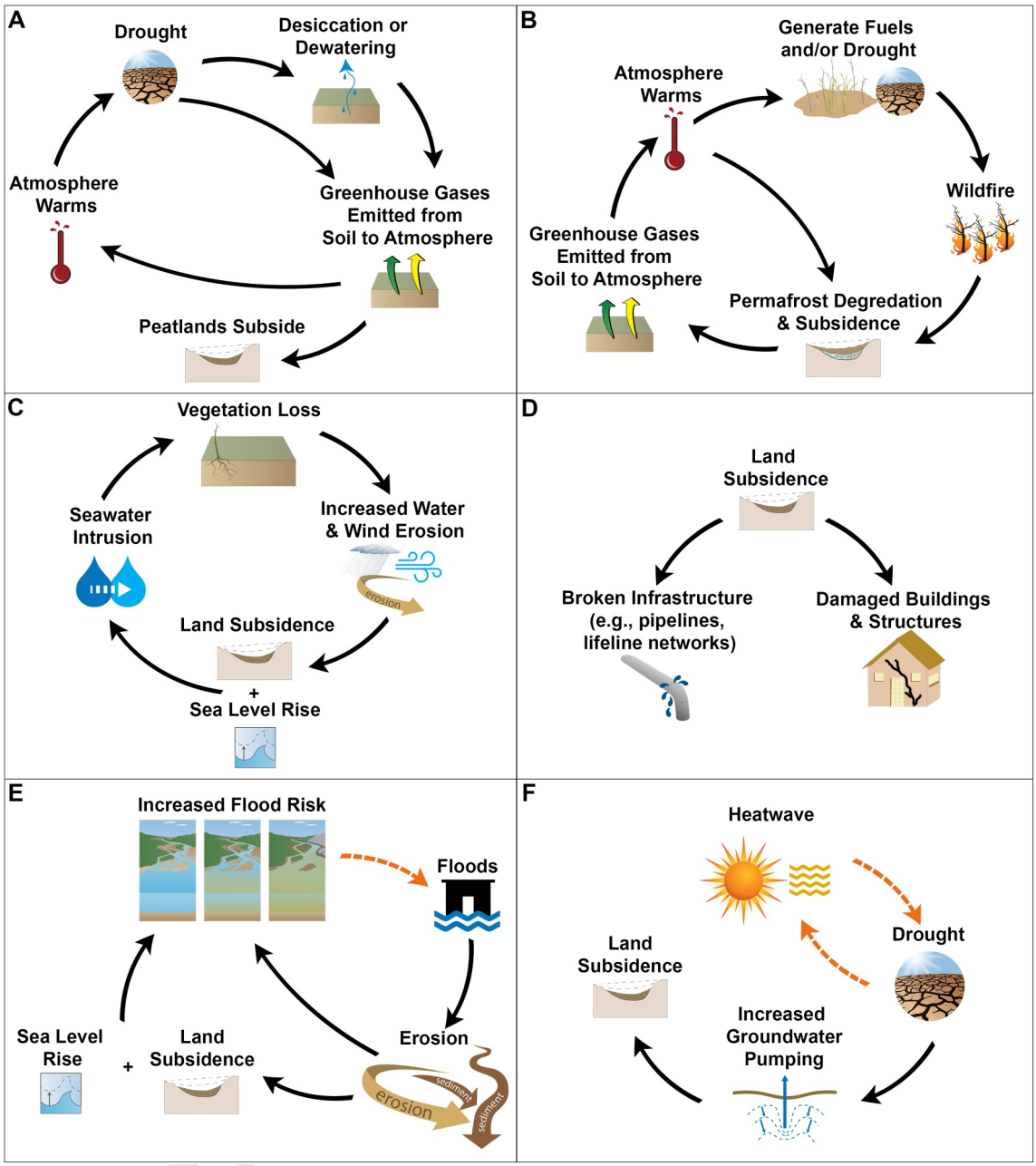

Figure 4. Land subsidence feedback loops and cascading hazards involving extreme events, climate change, and infrastructure. Feedbacks: (a) peatland-carbon, (b) permafrost-carbon, and (c) salinization-subsidence. Cascading hazards: (d) infrastructure-subsidence, (e) flood-subsidence, and (f) drought-subsidence. Black arrows indicate positive feedback. Orange dashed arrows indicate enhancement of impacts.

occurrence and severity of nuisance flooding (Sherpa et al., 2023; Sweet et al., 2014)—minor floods that do not pose major threats to public safety, but cause frequent disruption and urban inundation (Moftakhari et al., 2018). The combination of ongoing local LS and regional SLR will likely enhance coastal and tidal flooding from high tides and storm surges, leading to short-term sea level increases by several meters (Cooper et al., 2008; Syvitski et al., 2009; Wahl et al., 2015). The 2008 Cyclone Nargis storm surge flooded the lowlands of the Irrawaddy Delta (Myanmar) up to 6 m above sea level (Syvitski et al., 2009). The abovementioned hazards may compound to expand episodically flooded land, perpetual coastline loss from erosion and/or inundation of lowlands, and salinization of inland freshwater and soil (Cooper et al., 2008; Shirzaei & Bürgmann, 2018) (Figures 4c and 4e).

Such potential impacts are anticipated in Asian deltaic megacities (e.g., Manila, Tokyo, Ho Chi Minh City, Jakarta) (Cao et al., 2021; Colombani et al., 2016; IPCC, 2021).

The drainage of tropical coastal peatlands in southeast Asia causes communities to face many of these same hazards from subsidence and oxidation of peat (and greenhouse gas emissions), loss of productive land, and flooding since most of these areas are near sea level (Hoyt et al., 2020). Low-lying coastal regions are also often vulnerable to saline intrusion (J. Chen & Mueller, 2018), as detailed in Section 7.2. Furthermore, the compounding effects of SLR and the changing distribution and severity of climate change fueled-extremes on LS (Knutson et al., 2010; Vitousek et al., 2017) may increase the frequency of a given magnitude flood. Therefore, existing flood control infrastructure (e.g., levees, dikes, flood walls) is hypothesized to become effectively "under-designed" for the future 100- or 500-year flood of a larger magnitude than historically estimated (Buchanan et al., 2016; IPCC, 2021).

5.2. Droughts

Globally, groundwater overdraft, induced by drought and large water demands for agricultural and domestic uses, contributes to LS (Famiglietti, 2014; Faunt et al., 2016; Ghorbani et al., 2022; Richey et al., 2015) (Figure 4f). Heatwaves further compound societal and environmental stresses to enhance the effects of droughts (AghaKouchak et al., 2020; Mazdiyasni & AghaKouchak, 2015). Substantial groundwater level declines were observed during the multiyear droughts in the 1990s, 2000s, 2007–2010, and 2012–2016 in California's irrigated agricultural San Joaquin Valley (Smith & Knight, 2019). The latter two droughts across the region led to significant increases in groundwater pumping, causing highly variable subsidence (rates and cumulative magnitudes) (Faunt et al., 2016; Jeanne et al., 2019; Levy et al., 2020; Miller et al., 2020) because of factors such as subsurface hydrostratigraphy, despite similar water volumes extracted during both droughts (Smith & Knight, 2019). Drought induced abrupt subsidence adjacent to the California Aqueduct that supports the state's Central Valley agriculture and millions of people in southern California (Miller et al., 2020). Within a 112-day period amidst the drought in summer 2014, the 1-ha area experiencing 10–15 cm of elevation decline increased to 1,287 ha, and by 2016, a maximum cumulative displacement of 70–75 cm occurred along the aqueduct (Miller et al., 2020). Conveyance systems generally require costly retrofitting and repairing from LS (e.g., sealing leaks, restoring capacity, raising linings and embankments), to avoid overtopping, erosion, and delivery outages. Water conveyance and flood control systems throughout the region face such ongoing challenges (Faunt et al., 2016). Notwithstanding observed increasing groundwater levels and precipitation, subsidence may continue for years after drought termination (i.e., residual compaction) (Neely et al., 2021; Ojha et al., 2020). From 1999 to 2012, drought caused significant groundwater level decline and subsidence in Beijing; however, subsidence could not be definitively attributed to increased pumping rates, but rather correlated with groundwater storage anomalies resulting from low levels of precipitation and recharge (Gong et al., 2018). Since droughts can contribute to LS, which subsequently increases the flood risk for a region, this implies that impacts from one extreme or hazard have the potential to influence the risk of the "opposite" hazard (Ward et al., 2020).

6. Climate Feedbacks and Infrastructure Damage

6.1. Peatlands and Oxidation of Soil Organic Carbon and Matter

Peatlands comprise only about 3% of the Earth's land surface (Kaat & Joosten, 2009), but possess the largest natural terrestrial carbon storage containing over 550 gigatonnes of carbon, or 42% of all soil carbon (Cris et al., 2014). Anthropogenic activities and growing demands for land and cultivation have drained about 15% of the world's peatlands for agriculture or forestry (Cris et al., 2014), causing major CO_2 emissions from peatlands to the atmosphere and subsidence (Qiu et al., 2021). Primary causes of subsidence in organic soils and peatlands are grouped into five categories: (a) compaction and shrinkage of soil above the groundwater table from drainage or the application of heavy loads on the ground surface, (b) consolidation of saturated organic soil below the groundwater table from loss of buoyancy, (c) water and wind erosion, (d) microbial oxidation of soil organic matter (SOM) or soil organic carbon (SOC) decomposing peat above the groundwater table through breakdown of organic matter, and (e) burning (Deverel et al., 2016; Hooijer et al., 2012; Robinson & Vahedifard, 2016; Vahedifard et al., 2016). Records of subsidence in organic soils and peatlands span the globe including North America, Europe (e.g., the Netherlands, Italy, Russia, England, Norway), southern Asia (e.g., Indonesia,

Malaysia), Middle East (Israel), and Oceania (New Zealand) (Deverel et al., 2016; Erkens et al., 2016; Hooijer et al., 2012; Hoyt et al., 2020; Pronger et al., 2014).

Oxidation of SOM is recognized as a key factor causing subsidence in many deltas and peatlands worldwide. Microbial oxidation of SOM is reported to account for approximately 75% and 53% of historic subsidence in the Sacramento-San Joaquin Delta, California (Mount & Twiss, 2005) and Everglades peats, Florida (Stephens et al., 1984) (USA), respectively. In tropical peatlands of southern Asia, 75% and 92% of total subsidence after 5 and 18 years of drainage, respectively, was caused by oxidation of SOM (Hooijer et al., 2012). In the Netherlands, at least 70% of the human-induced subsidence is attributed to oxidation of SOM (Den Haan & Kruse, 2006). While other factors trigger subsidence (e.g., shrinkage, consolidation), oxidation is the only mechanism that causes CO_2 emission to the atmosphere (Erkens et al., 2016). Oxidation of SOM represents a central coupling between LS and the climate system that is expected to accelerate climate change (IPCC, 2019) (Figure 4a). Furthermore, as the climate warms and leads to more severe droughts, vegetation and soil may become stressed. The heightened stress can enhance soil desiccation cracking that causes greater exposure of soil carbon to oxidation, and thereby, amplifies climate change by increasing greenhouse gas emissions from the soil to the atmosphere (Vahedifard, Goodman, et al., 2024). Thus, these processes give rise to an amplifying feedback loop. If such feedbacks are overlooked, inaccuracies in modeling and predicting greenhouse gas emissions from soils may cause us to underestimate important climate change impacts on soil and crop health, the structural integrity of earthen infrastructure systems, and the acceleration of LS (Vahedifard, Goodman, et al., 2024).

Anthropogenic climate change and land use and land cover change can trigger greater subsidence in organic soils and peatlands by accelerating microbial oxidation of SOC in these soils. Climate change-induced changes in soil temperature and moisture greatly alter SOC dynamics. With their high activation energies (i.e., slow rates), organic soils undergo larger proportional increases in decomposition with rising temperature (Conant et al., 2011; Davidson & Janssens, 2006). This implies that prolonged droughts can induce larger subsidence not only through creating higher demands for more groundwater extraction (triggering deep subsidence), but also through increasing the decomposition rates of SOC (triggering shallow subsidence) (Vahedifard et al., 2016). Furthermore, preservation of the organic-rich peatlands, often found in wetlands, is important for ecosystem services in disaster risk management and infrastructure protection. In fact, U.S. coastal wetlands provide an estimated $23.2 billion annually through storm protection services, for example, reducing flooding from hurricanes, which is valued at $8,240/ha/yr (Costanza et al., 2008). These areas should be valued significantly higher if their role in the carbon budget were included (Dean et al., 2018). As wetlands are drained, this causes oxygen to move into deeper layers of the soil. This leads to aerobic activity that decomposes the organic matter, leading to LS with large carbon dioxide emissions from the soil into the atmosphere. As a result, these drained and degraded peatlands become net carbon sources that feedback into the climate system to cause further atmospheric warming and enhance this cycle (Dean et al., 2018). Moreover, the loss of wetlands is exacerbated by the compounding effects of LS and SLR (Ohenhen et al., 2023). The preservation of wetlands as well as subsidence rates in these regions are influenced by climate factors such as rainfall and human interventions such as dams that affect the functionality of the wetlands by altering the sediment supply and transport to these areas (Ganju et al., 2015; Z. Liu et al., 2021).

6.2. Critical Infrastructure

Monitoring the proximity of subsidence to critical infrastructure is crucial since infrastructure damage can result in loss of life and critical lifeline failures/outages (e.g., water conveyance, transportation, and utility systems) (Ge et al., 2010; Miller et al., 2020) (Figure 4d). The interaction between LS and infrastructure is exemplified by the levee failures in New Orleans, Louisiana during Hurricane Katrina in 2005, which caused over 1,300 deaths and more than $100 billion in economic loss (Briaud et al., 2008). A 2002–2005 period of LS gave rise to the overtopping failures of the levee system during the hurricane's peak storm surge (Dixon et al., 2006). Uniform and differential settlements induced by subsidence degrade the functionality and integrity of infrastructure at element (e.g., foundations, structural components, utility) and system scales. LS has been reported to cause considerable damage to buildings and lifeline infrastructure systems such as pipelines (Baum et al., 2008), roads (Shi et al., 2018), railways (Li et al., 2021), bridges (B. Chen et al., 2021), electric power network systems (Tzampoglou & Loupasakis, 2018), and irrigation and drainage systems (Abidin et al., 2015). Leaking water, oil, or sewage from a pipe or drain, ice/snow melt, or precipitation can also trigger subsidence of unstable media, further damaging infrastructure. Long-term leaky pipelines or a sudden water main burst may cause or be caused by LS.

This occurs when the fluid erodes the underlying soil foundation or compresses/weakens soils such that they are no longer able to support the overlying structural load, resulting in subsidence and additional infrastructure damage (Marker, 2013).

Human activities (e.g., infrastructure expansion and development) and climate change amplify permafrost thaw during warm periods, leading to infrastructure damage and failures (Hjort et al., 2022; Shiklomanov et al., 2017). The impacts of land degradation on infrastructure underlain by permafrost or perennially frozen ground place food security, livelihoods, and cultural traditions at risk (Gibson et al., 2021). With over two-thirds of Russia underlain by permafrost, several examples of infrastructure damage exist across the country (e.g., Norilsk, Vorkuta), where warming is nearly three times faster than the global average with climate change (Shiklomanov et al., 2017; Streletskiy et al., 2015). In Arctic Russia, bearing capacity declines up to 40% from the 1960s–2000s were measured in urban areas where the formation of the uneven thermokarst topography and thawed layers are common (Hjort et al., 2022). Thawing frozen ground has also left up to 30% of the road embankments in the Qinghai-Tibet Plateau experiencing permafrost-related damage (Hjort et al., 2022).

6.3. Wildfires and Permafrost Thaw

Wildfires in permafrost areas can trigger LS by altering the surface albedo, thawing the permafrost layer through heat exposure, and removing vegetation cover (Vahedifard, Abdollahi, et al., 2024; Yanagiya & Furuya, 2020). Following a 2014 wildfire across an ice-rich permafrost region near Batagay, Eastern Siberia, the 1-year maximum subsidence of 10 cm or more was observed where permafrost thawed and thermokarst formations developed (Yanagiya & Furuya, 2020). By the second post-fire thawing season, fire-induced permafrost degradation of up to 20 cm of subsidence was estimated and deepening of the active layer of up to 80 cm 2 years post-fire in the boreal forests in Yukon Flats, Alaska (USA) (Eshqi Molan et al., 2018). When LS and thermokarst exhibit greater heterogeneity than the burn severity, this poses challenges for relating burn characteristics and subsidence (Yanagiya & Furuya, 2020). Roughly half of the world's northern peatland regions are underlain by permafrost with an estimated 50% of the globe's peatland carbon stored within 60–70°N (Hugelius et al., 2020). Since the regrowth of burnt peatlands is a slow process, the released carbon has significant long-term global climate effects (Witze, 2020). Thus, thawing ice-rich permafrost releases large amounts of greenhouse gases stored in the frozen subsurface (Figure 4b) changing these regions from carbon sinks to sources and promoting global warming (Dean et al., 2018). Snow thickness and albedo, among other factors, greatly influence the temperature of permafrost (Streletskiy et al., 2015). Hence, declines in snow cover and shorter snow seasons could lead to the warming of permafrost, its degradation, and subsidence.

7. Climate Change-Fueled Future Risks and Vulnerabilities

7.1. Sea Level Rise

LS projections are inherently coupled to the climate system and human activities. By 2040, the projected potential subsidence areas will increase by 7%, while a 30% rise in the population affected by subsidence is expected (Herrera-García et al., 2021) due to many compounding factors, including human migration and urbanization, intensification of droughts, changes in land cover and land use, SLR, and overall warming temperatures (Figure 3). High population density in coastal areas accelerates compaction and human-induced subsidence (mainly groundwater-driven) and consequently, local SLR much higher than climate-induced SLR (Nicholls et al., 2021). Also, upstream reduction of active tributaries and increased infrastructure development prevent sediment redistribution and delta aggradation, which contribute to sinking rates that exceed regional SLR (Shirzaei et al., 2021; Syvitski et al., 2009; Tessler et al., 2015). Despite challenges in predicting basin management and infrastructure investments, the frequency of flooding is estimated to double across most of the U.S. shoreline (Shirzaei et al., 2021) and deltas vulnerable to flooding could increase by at least 50% by 2100 (Syvitski et al., 2009; Tessler et al., 2015) from compounding LS rates and SLR. By 2050, projections based solely on socioeconomic change raise the average global flood losses to $52 billion/yr, and with projected subsidence and SLR rates included, losses would further increase by $8–11 billion/yr even if adaptation strategies maintained current flood probabilities (Hallegatte et al., 2013). Population growth in dry/arid climates is also expected to strain available freshwater sources from increased demand and precipitation seasonality in such climate zones.

Current global estimates indicate that irrigated areas cover about 300 Mha and irrigation water accounts for over 90% of the global water consumption (AghaKouchak et al., 2021; Hoekstra & Mekonnen, 2012;

Siebert et al., 2015). As the global population grows, the corresponding demand for agricultural products and irrigation water will also rise (Qin et al., 2020; Tilman et al., 2011; Wada et al., 2011). This is compounded by shifts in evaporative losses, runoff and snowmelt magnitude and timing, and shrinkage of existing surface water bodies, causing greater reliance on alternative water supplies such as groundwater (Huning & AghaKouchak, 2018, 2020; IPCC, 2021; Qin et al., 2020; Rodell et al., 2018; Siirila-Woodburn et al., 2021; Wada & Bierkens, 2014) that may exacerbate subsidence in overdrawn groundwater aquifers. Intensified droughts decrease groundwater levels from reduced recharge via precipitation and cause increased pumping that enhances subsidence in overdrawn aquifers (Figure 4). Future groundwater-related subsidence estimates are thereby complicated by uncertain precipitation projections from climate models (IPCC, 2021; Langenbrunner et al., 2015; Shen et al., 2018). Nonetheless, projections suggest that dry areas will become drier while wet areas will become wetter (Greve et al., 2014; Hao et al., 2018; IPCC, 2021; Padrón et al., 2020). Also, climate change-induced acceleration of the terrestrial water cycle increases floods and droughts across many regions (AghaKouchak et al., 2020; Chagas et al., 2022; IPCC, 2021).

7.2. Water Quality and Environmental Effects of Salinization

Climate change is hypothesized to also contribute to water quality issues through salinization of ground and surface water (Figure 4c) from SLR and/or LS in coastal regions (Colombani et al., 2016). As soils and water sources become saltier, this often alters nutrient dynamics, increases environmental stress, and reduces SOM, leading to further subsidence and challenges for maintaining water and food security (Ullah et al., 2021). If vegetation cannot survive under saline conditions and protect the soil, wind and water may cause erosion, decreasing the ground elevation (Hassani et al., 2021). Furthermore, "ghost forests" develop in low-lying coastal areas when saltwater intrudes with rising sea levels and poisons the freshwater-dependent, living trees. As the seawater intrudes, it leaves dead and dying standing trees or a ghost forest as these regions transform into more salt-tolerant marshes or wetlands (Kirwan & Gedan, 2019; Smart et al., 2020). Additional LS occurs as the roots of these trees rot. In agricultural areas with saline soils, lost income has spurred migration and urbanization (J. Chen & Mueller, 2018), which commonly contributes to subsidence. Salinization from metallurgy activities also occurs in other regions, including permafrost areas such as Norilsk (Russia), where soil salinization decreases the stability of infrastructure by reducing the freezing temperature of soil, lowering the likelihood of permafrost recovery especially with climate change, and corroding building materials in the active layer (Streletskiy et al., 2015). It is challenging to project salinization extent from human activities since salinization occurs from one or multiple uncertain/variable drivers.

7.3. Permafrost, Peatlands, and Climate Feedbacks

As Arctic temperatures warm across permafrost regions, it is anticipated that areas experiencing thermokarst formation and thaw-driven subsidence will expand. Projections indicate that by mid-century, the thawing and loss of permafrost will affect an estimated 3.3 million people in the Arctic with 42% of settlements on permafrost becoming permafrost-free zones (Ramage et al., 2021). By this time, models project losses of 20%–33% of the permafrost environment and more than 50% on average with unmitigated emission scenarios by 2061–2080 (Karjalainen et al., 2020). As much as 50% of the Arctic infrastructure is expected to be at high-risk for damage from permafrost thaw by 2050 (Hjort et al., 2022). Future permafrost recovery, however, is not well-estimated since thermokarst is generally neglected in models (Holloway et al., 2020). Nonetheless, it is well-known that differential subsidence causes cracking and buckling of structures and roadways. By the mid-to-late twenty-first century, infrastructure costs from permafrost degradation could total to tens of billions of dollars (Hjort et al., 2022).

Permafrost loss will also affect biogeochemical processes, hydrology, biodiversity, and global climate (Karjalainen et al., 2020). Therefore, considering thermokarst-inducing processes and permafrost degradation is important for estimating thaw-affected carbon release (Figure 4b), which by 2100 could be 3 to 12-fold of what is currently projected in the northeast Siberian Arctic lowlands (Nitzbon et al., 2020). Moreover, larger and more severe wildfires combined with the warmer and longer fire seasons in boreal and tundra regions accelerate the melting of ground ice more than would be expected from warming effects alone (Gibson et al., 2018; Holloway et al., 2020). Wildfires deepen the active layer and expand talik areas with effects persisting or being delayed for decades afterward. Peatlands of northwestern Canada saw increases of continuously thawed soil layers or taliks of 70%–100% in burned areas 10–20 years after fires compared to increases of only 20% in unburned areas

(Gibson et al., 2018). Since permafrost recovery must contend with a warming climate and extremes (e.g., wildfires, heatwaves), this leads to slower recoveries (if at all), which also may cause more talik and thermokarst development, warmer deep soil temperatures, and greater future subsidence (Holloway et al., 2020).

Overall, LS is a global, multi-faceted issue that affects people, infrastructure, and ecosystems beyond local impacts. When viewed within the larger context of the climate, LS couplings (Figures 3 and 4) have the potential to impact remote regions (e.g., via migration, resource competition, agricultural productivity, climate change).

8. Research Gaps and Opportunities

Our global community must recognize the urgency of mitigating, and where possible, reversing anthropogenic LS. Subsidence-related policies, regulations, and mitigation measures tend to be reactive rather than proactive due to the complexity of this chronic hazard, which often goes unnoticed initially as sinking occurs slowly (Kondolf et al., 2022; Ohenhen, Shirzaei, & Barnard, 2024; Oppenheimer et al., 2019; Siriwardane-de Zoysa et al., 2021). Human perception of risk significantly influences the characterization and evaluation of LS, impacting the speed and manner in which adaptation, mitigation strategies, and public policies are formulated worldwide to address LS hazards and their repercussions. Furthermore, perception of risk to LS has contributed to LS not becoming a proactive public policy topic in many regions of the world (Dinar et al., 2021; Siriwardane-de Zoysa et al., 2021). Therefore, rather than LS being viewed as a purely "technical" or "scientific" issue, as commonly occurs, LS consideration must be integrated into societal policies and decisions (Batubara et al., 2023). Additionally, significant, yet highly localized subsidence is frequently overlooked if monitoring solely relies on limited point observations (Levy et al., 2020). If the spatial variability of LS is not well-represented in models, estimates of future exposure to flooding will likely be inaccurate, meaning that communities may be ill-prepared and misinformed when developing and implementing adaptation and mitigation strategies (Ohenhen, Shirzaei, Ojha, et al., 2024). In spite of major advances in monitoring and modeling subsidence and impacts, continued technological, engineering, and policy advancements must be coupled with adaptation strategies to avoid intensifying climate change and heightening flood risks to large populations, water quality issues, etc. from subsidence-related disasters. Namely, we must leverage the often-undervalued ecological services that peatlands play in reducing damage to infrastructure and loss of life, and mitigating climate change.

Currently, we lack models and tools for developing holistic adaptation and mitigation strategies. Additional research is still needed to develop high-resolution LS maps at scales necessary for management, adaptation, mitigation, and policy (Levy et al., 2020; Shirzaei et al., 2021). Most of the processes described here do not operate in isolation; therefore, for reasonable management-scale outcomes, neither should our models. Model projections of subsidence are complicated by trying to predict the interconnected anthropogenic sources and locations of LS, which are layered on top of natural causes (Gambolati et al., 2005). Integrated models that incorporate multiple drivers and processes are required to fully understand the magnitude of subsidence and its interplay with population, infrastructure, climate change, and other hazards. Anthropogenic subsidence and related feedbacks (sediment dynamics, carbon cycle, climate extremes as in Figure 4, etc.) must be accounted for in studies related to projected SLR and future flooding risks (Oppenheimer et al., 2019; Shirzaei & Bürgmann, 2018; Shirzaei et al., 2021), and particularly in coastal and urban areas given their potential costly socioeconomic and environmental implications. Climate simulations should account for increased wildfire frequency when estimating subsidence in permafrost and permafrost-free peatlands (Gibson et al., 2018). Since climate models do not represent abrupt permafrost thaw, the magnitude and rate of carbon emissions, and the acceleration of climate change, are hypothesized to differ from current large-scale model estimates (Turetsky et al., 2020). Yet, these are non-trivial modeling tasks that cannot be accomplished without additional observational analyses, basic research, and integrated, more detailed process understandings. In addition, many regions around the world face challenges from inadequate access to accurate data and/or technological resources for collecting data related to LS rates, drivers, impacts, and climate feedbacks (Avornyo et al., 2024; Nicholls & Shirzaei, 2024). Therefore, collecting additional data across the globe and in particular, in data scarce regions, will be highly beneficial.

Hence, efforts to compile and maintain longer observational and spatially distributed records remain necessary. Data fusion, data assimilation, and machine learning are examples of methods that facilitate integrating information from various data streams together (e.g., Davydzenka et al., 2024); however, combining measurements from different satellite and observational sources poses challenges where instruments, measurement types, record

lengths, and spatiotemporal resolutions differ. While progress has been made in this area, we lack multi-sensor, composite, and spatially consistent subsidence estimates. Such a data set will help constrain models and inform further investigations of complex LS-climate couplings and adaptation and mitigation strategies.

Many questions and gaps still remain related to integrating climate, extremes, and human drivers with overall subsidence as our review presents. Further studies are needed to better quantify the effects of temperature rise due to climate change on the decomposability and response rates of SOC. Our current understanding is limited about how much carbon is stored deep in alluvial soil profiles, for example, >1 m below the surface, and how susceptible the carbon is to oxidation. It is often understood that this pool of carbon is much older, more stable, and more protected from oxidation. Also, many existing terrestrial ecosystem models do not consider these deeper pools. So, a key question is: what effects will protracted drought and drought-induced deep cracking of soils have on these deep SOC pools and subsequent LS? Furthermore, while it is understood that heatwaves amplify droughts and hence soil cracking, to what extent does this translate into deeper soil carbon reserves being accessed in peatlands and permafrost? Also, to what extent do compounding heatwaves and droughts heighten groundwater depletion and subsidence? What heatwave frequency, severity, and duration can increase the active zone in permafrost regions leading to irreversible impacts of subsidence? What are the implications of rapid versus gradual thaw of permafrost on subsidence, climate change, and the positive carbon feedback? Beyond permafrost regions, what role do wildfires play in LS?

We urge the community to build upon work from other fields (e.g., drought monitoring application/literature (Mishra & Singh, 2010; Svoboda & Fuchs, 2016)) to develop a severity scale, associated subsidence indices, and/or a subsidence monitor/database. The establishment of common globally accepted approaches would provide a consistent framework for better understanding the measured and reported rates and identifying at-risk communities and effective mitigation strategies. Risk mitigation cannot be outpaced by exposure. Interdisciplinary, synergistic collaborations should be forged to develop more reliable global subsidence monitoring and translate observations and modeling into actionable strategies for hazard/risk mitigation, resource management, climate resilience, engineering design, urban planning, and sustainable policy. International organizations such as UNESCO already recognize the earnestness of land deformation issues with the development of their "Land Subsidence International Initiative" for globally mapping subsidence (UNESCO, n.d.). To better inform the abovementioned strategies and initiatives, and prioritize vulnerable areas, advancements in predicting future LS at a variety of spatiotemporal scales and under different conditions related to climate, hydrologic anomalies, water/resource demands, urbanization, etc. must be made (Smith & Knight, 2019). Process-based integrated management modeling from the atmosphere to bedrock would benefit LS research, but also require a concerted effort across disciplines and sectors.

Data Availability Statement

All data is available from published sources (see Supporting Information S1).

Acknowledgments
This work was partially supported by the University of California, Division of Agriculture and Natural Resources California Institute for Water Resources and U.S. Geological Survey Grant G21AP10611-00, National Science Foundation award numbers CMMI-2332263, CBET-2301815, OAC-1931335, and OISE-2114701, Department of Energy Grant DE-SC0023539, and California State University Water Resources and Policy Initiatives grant. Symbols courtesy of the Integration and Application Network (https://ian.umces.edu/symbols), were adopted or modified in Figure 4.

References

Abidin, H. Z., Andreas, H., Gumilar, I., & Brinkman, J. J. (2015). Study on the risk and impacts of land subsidence in Jakarta. *Proceedings of the International Association of Hydrological Sciences*, *372*, 115–120. https://doi.org/10.5194/piahs-372-115-2015

AghaKouchak, A., Chiang, F., Huning, L. S., Love, C. A., Mallakpour, I., Mazdiyasni, O., et al. (2020). Climate extremes and compound hazards in a warming world. *Annual Review of Earth and Planetary Sciences*, *48*(1), 519–548. https://doi.org/10.1146/annurev-earth-071719-055228

AghaKouchak, A., Mirchi, A., Madani, K., Di Baldassarre, G., Nazemi, A., Alborzi, A., et al. (2021). Anthropogenic drought: Definition, challenges, and opportunities. *Reviews of Geophysics*, *59*(2), e2019RG000683. https://doi.org/10.1029/2019RG000683

Aly, M. H., Zebker, H. A., Giardino, J. R., & Klein, A. G. (2009). Permanent scatterer investigation of land subsidence in Greater Cairo, Egypt. *Geophysical Journal International*, *178*(3), 1238–1245. https://doi.org/10.1111/j.1365-246X.2009.04250.x

Ao, M., Wang, C., Xie, R., Zhang, X., Hu, J., Du, Y., et al. (2015). Monitoring the land subsidence with persistent scatterer interferometry in Nansha District, Guangdong, China. *Natural Hazards*, *75*(3), 2947–2964. https://doi.org/10.1007/s11069-014-1471-2

Ao, Z., Hu, X., Tao, S., Hu, X., Wang, G., Li, M., et al. (2024). A national-scale assessment of land subsidence in China's major cities. *Science*, *384*(6693), 301–306. https://doi.org/10.1126/science.adl4366

Arnell, N. W. (2004). Climate change and global water resources: SRES emissions and socio-economic scenarios. *Global Environmental Change*, *14*(1), 31–52. https://doi.org/10.1016/j.gloenvcha.2003.10.006

ASCE Land Subsidence Task Committee. (2022). *Investigation of land subsidence due to fluid withdrawal*. American Society of Civil Engineers. https://doi.org/10.1061/9780784415702

Avornyo, S. Y., Minderhoud, P. S. J., Teatini, P., Seeger, K., Hauser, L. T., Woillez, M.-N., et al. (2024). The contribution of coastal land subsidence to potential sea-level rise impact in data-sparse settings: The case of Ghana's Volta delta. *Quaternary Science Advances*, *14*, 100175. https://doi.org/10.1016/j.qsa.2024.100175

Awasthi, S., Jain, K., Bhattacharjee, S., Gupta, V., Varade, D., Singh, H., et al. (2022). Analyzing urbanization induced groundwater stress and land deformation using time-series Sentinel-1 datasets applying PSInSAR approach. *Science of the Total Environment*, *844*, 157103. https://doi.org/10.1016/j.scitotenv.2022.157103

Baghdadi, N., Aubert, M., Cerdan, O., Franchistéguy, L., Viel, C., Eric, M., et al. (2007). Operational mapping of soil moisture using synthetic aperture radar data: Application to the Touch Basin (France). *Sensors*, *7*(10), 2458–2483. https://doi.org/10.3390/s7102458

Bagheri, M., Dehghani, M., Esmaeily, A., & Akbari, V. (2019). Assessment of land subsidence using interferometric synthetic aperture radar time series analysis and artificial neural network in a geospatial information system: Case study of Rafsanjan Plain. *Journal of Applied Remote Sensing*, *13*(04), 1. https://doi.org/10.1117/1.JRS.13.044530

Bagheri-Gavkosh, M., Hosseini, S. M., Ataie-Ashtiani, B., Sohani, Y., Ebrahimian, H., Morovat, F., & Ashrafi, S. (2021). Land subsidence: A global challenge. *Science of the Total Environment*, *778*, 146193. https://doi.org/10.1016/j.scitotenv.2021.146193

Batubara, B., Kooy, M., & Zwarteveen, M. (2023). Politicising land subsidence in Jakarta: How land subsidence is the outcome of uneven sociospatial and socionatural processes of capitalist urbanization. *Geoforum*, *139*, 103689. https://doi.org/10.1016/j.geoforum.2023.103689

Baum, R., Galloway, D. L., & Harp, E. L. (2008). *Landslide and land subsidence hazards to pipelines (Open-File Report No. 2008–1164)*. USGS.

Blum, M. D., Tomkin, J. H., Purcell, A., & Lancaster, R. R. (2008). Ups and downs of the Mississippi Delta. *Geology*, *36*(9), 675. https://doi.org/10.1130/G24728A.1

Bockstiegel, M., Richard-Cerda, J. C., Muñoz-Vega, E., Haghighi, M. H., Motagh, M., Lalehzari, R., & Schulz, S. (2023). Simulation of present and future land subsidence in the Rafsanjan plain, Iran, due to groundwater overexploitation using numerical modeling and InSAR data analysis. *Hydrogeology Journal*, *32*(1), 289–305. https://doi.org/10.1007/s10040-023-02657-y

Bonì, R., Meisina, C., Teatini, P., Zucca, F., Zoccarato, C., Franceschini, A., et al. (2020). 3D groundwater flow and deformation modelling of Madrid aquifer. *Journal of Hydrology*, *585*, 124773. https://doi.org/10.1016/j.jhydrol.2020.124773

Briaud, J.-L., Chen, H.-C., Govindasamy, A. V., & Storesund, R. (2008). Levee erosion by overtopping in New Orleans during the Katrina Hurricane. *Journal of Geotechnical and Geoenvironmental Engineering*, *134*(5), 618–632. https://doi.org/10.1061/(ASCE)1090-0241(2008)134:5(618)

Bru, G., Herrera, G., Tomás, R., Duro, J., De la Vega, R., & Mulas, J. (2013). Control of deformation of buildings affected by subsidence using persistent scatterer interferometry. *Structure and Infrastructure Engineering*, *9*(2), 188–200. https://doi.org/10.1080/15732479.2010.519710

Brunori, C. A., Bignami, C., Zucca, F., Groppelli, G., Norini, G., Davila Hernández, N., & Stramondo, S. (2015). Ground fracturation in urban area: Monitoring of land subsidence controlled by buried faults with InSAR techniques (Ciudad Guzmán: Mexico). In G. Lollino, A. Manconi, F. Guzzetti, M. Culshaw, P. Bobrowsky, & F. Luino (Eds.), *Engineering geology for society and territory* (Vol. 5, pp. 1027–1031). Springer International Publishing. https://doi.org/10.1007/978-3-319-09048-1_196

Buchanan, M. K., Kopp, R. E., Oppenheimer, M., & Tebaldi, C. (2016). Allowances for evolving coastal flood risk under uncertain local sea-level rise. *Climatic Change*, *137*(3–4), 347–362. https://doi.org/10.1007/s10584-016-1664-7

Bürgmann, R., Rosen, P. A., & Fielding, E. J. (2000). Synthetic aperture radar interferometry to measure Earth's surface topography and its deformation. *Annual Review of Earth and Planetary Sciences*, *28*(1), 169–209. https://doi.org/10.1146/annurev.earth.28.1.169

Calderhead, A. I., Therrien, R., Rivera, A., Martel, R., & Garfias, J. (2011). Simulating pumping-induced regional land subsidence with the use of InSAR and field data in the Toluca Valley, Mexico. *Advances in Water Resources*, *34*(1), 83–97. https://doi.org/10.1016/j.advwatres.2010.09.017

Cao, A., Esteban, M., Valenzuela, V. P. B., Onuki, M., Takagi, H., Thao, N. D., & Tsuchiya, N. (2021). Future of Asian deltaic megacities under sea level rise and land subsidence: Current adaptation pathways for Tokyo, Jakarta, Manila, and Ho Chi Minh City. *Current Opinion in Environmental Sustainability*, *50*, 87–97. https://doi.org/10.1016/j.cosust.2021.02.010

Carminati, E., & Martinelli, G. (2002). Subsidence rates in the Po Plain, northern Italy: The relative impact of natural and anthropogenic causation. *Engineering Geology*, *66*(3–4), 241–255. https://doi.org/10.1016/S0013-7952(02)00031-5

Castellazzi, P., Martel, R., Galloway, D. L., Longuevergne, L., & Rivera, A. (2016). Assessing groundwater depletion and dynamics using GRACE and InSAR: Potential and limitations. *Groundwater*, *54*(6), 768–780. https://doi.org/10.1111/gwat.12453

Catalao, J., Nico, G., Lollino, P., Conde, V., Lorusso, G., & Silva, C. (2016). Integration of InSAR analysis and numerical modeling for the assessment of ground subsidence in the City of Lisbon, Portugal. *IEEE Journal of Selected Topics in Applied Earth Observations and Remote Sensing*, *9*(4), 1663–1673. https://doi.org/10.1109/JSTARS.2015.2428615

Chagas, V. B. P., Chaffe, P. L. B., & Blöschl, G. (2022). Climate and land management accelerate the Brazilian water cycle. *Nature Communications*, *13*(1), 5136. https://doi.org/10.1038/s41467-022-32580-x

Chaussard, E., Amelung, F., Abidin, H., & Hong, S.-H. (2013). Sinking cities in Indonesia: ALOS PALSAR detects rapid subsidence due to groundwater and gas extraction. *Remote Sensing of Environment*, *128*, 150–161. https://doi.org/10.1016/j.rse.2012.10.015

Chaussard, E., Havazli, E., Fattahi, H., Cabral-Cano, E., & Solano-Rojas, D. (2021). Over a century of sinking in Mexico City: No hope for significant elevation and storage capacity recovery. *Journal of Geophysical Research: Solid Earth*, *126*(4), e2020JB020648. https://doi.org/10.1029/2020JB020648

Chen, B., Gong, H., Chen, Y., Lei, K., Zhou, C., Si, Y., et al. (2021). Investigating land subsidence and its causes along Beijing high-speed railway using multi-platform InSAR and a maximum entropy model. *International Journal of Applied Earth Observation and Geoinformation*, *96*, 102284. https://doi.org/10.1016/j.jag.2020.102284

Chen, F., Lin, H., Zhang, Y., & Lu, Z. (2012). Ground subsidence geo-hazards induced by rapid urbanization: Implications from InSAR observation and geological analysis. *Natural Hazards and Earth System Sciences*, *12*(4), 935–942. https://doi.org/10.5194/nhess-12-935-2012

Chen, J., & Mueller, V. (2018). Coastal climate change, soil salinity and human migration in Bangladesh. *Nature Climate Change*, *8*(11), 981–985. https://doi.org/10.1038/s41558-018-0313-8

Cigna, F., & Tapete, D. (2021). Present-day land subsidence rates, surface faulting hazard and risk in Mexico City with 2014–2020 Sentinel-1 IW InSAR. *Remote Sensing of Environment*, *253*, 112161. https://doi.org/10.1016/j.rse.2020.112161

Colombani, N., Osti, A., Volta, G., & Mastrocicco, M. (2016). Impact of climate change on salinization of coastal water resources. *Water Resources Management*, *30*(7), 2483–2496. https://doi.org/10.1007/s11269-016-1292-z

Conant, R. T., Ryan, M. G., Ågren, G. I., Birge, H. E., Davidson, E. A., Eliasson, P. E., et al. (2011). Temperature and soil organic matter decomposition rates—Synthesis of current knowledge and a way forward. *Global Change Biology*, *17*(11), 3392–3404. https://doi.org/10.1111/j.1365-2486.2011.02496.x

Cooper, M. J. P., Beevers, M. D., & Oppenheimer, M. (2008). The potential impacts of sea level rise on the coastal region of New Jersey, USA. *Climatic Change*, *90*(4), 475–492. https://doi.org/10.1007/s10584-008-9422-0

Costanza, R., Pérez-Maqueo, O., Martinez, M. L., Sutton, P., Anderson, S. J., & Mulder, K. (2008). The value of coastal wetlands for hurricane protection. *AMBIO: A Journal of the Human Environment*, *37*(4), 241–248. https://doi.org/10.1579/0044-7447(2008)37[241:TVOCWF]2.0.CO;2

R. Cris, S. Buckmaster, C. Bain, M. Reed, & H. Joosten (Eds.) (2014). *Global peatland restoration: Demonstrating success*. IUCN National Committee Peatland Programme.

Cruz, H., Véstias, M., Monteiro, J., Neto, H., & Duarte, R. P. (2022). A review of synthetic-aperture radar image formation algorithms and implementations: A computational perspective. *Remote Sensing*, *14*(5), 1258. https://doi.org/10.3390/rs14051258

Dang, V. K., Doubre, C., Weber, C., Gourmelen, N., & Masson, F. (2014). Recent land subsidence caused by the rapid urban development in the Hanoi region (Vietnam) using ALOS InSAR data. *Natural Hazards and Earth System Sciences*, *14*(3), 657–674. https://doi.org/10.5194/nhess-14-657-2014

Davidson, E. A., & Janssens, I. A. (2006). Temperature sensitivity of soil carbon decomposition and feedbacks to climate change. *Nature*, *440*(7081), 165–173. https://doi.org/10.1038/nature04514

Davydzenka, T., Tahmasebi, P., & Shokri, N. (2024). Unveiling the global extent of land subsidence: The sinking crisis. *Geophysical Research Letters*, *51*(4), e2023GL104497. https://doi.org/10.1029/2023GL104497

Dean, J. F., Middelburg, J. J., Röckmann, T., Aerts, R., Blauw, L. G., Egger, M., et al. (2018). Methane feedbacks to the global climate system in a warmer world. *Reviews of Geophysics*, *56*(1), 207–250. https://doi.org/10.1002/2017RG000559

Den Haan, E. J., & Kruse, G. A. M. (2006). Characterisation and engineering properties of Dutch peats, Ch. 13. In K. K. Phoon, D. W. Hight, & T. S. Tan (Eds.), *Characterisation and engineering properties of natural soils* (pp. 2101–2133). Taylor and Francis. https://doi.org/10.1201/NOE0415426916.ch13

Deverel, S. J., Ingrum, T., & Leighton, D. (2016). Present-day oxidative subsidence of organic soils and mitigation in the Sacramento-San Joaquin Delta, California, USA. *Hydrogeology Journal*, *24*(3), 569–586. https://doi.org/10.1007/s10040-016-1391-1

Dinar, A., Esteban, E., Calvo, E., Herrera, G., Teatini, P., Tomás, R., et al. (2021). We lose ground: Global assessment of land subsidence impact extent. *Science of the Total Environment*, *786*, 147415. https://doi.org/10.1016/j.scitotenv.2021.147415

Dixon, T. H., Ferretti, A., Novali, F., Rocca, F., Dokka, R., Sella, G., et al. (2006). Subsidence and flooding in New Orleans. *Nature*, *441*(7093), 587–588. https://doi.org/10.1038/441588a

Dong, S., Samsonov, S., Yin, H., Ye, S., & Cao, Y. (2014). Time-series analysis of subsidence associated with rapid urbanization in Shanghai, China measured with SBAS InSAR method. *Environmental Earth Sciences*, *72*(3), 677–691. https://doi.org/10.1007/s12665-013-2990-y

Du, Q., Chen, D., Li, G., Cao, Y., Zhou, Y., Chai, M., et al. (2023). Preliminary study on InSAR-based uplift or subsidence monitoring and stability evaluation of ground surface in the permafrost zone of the Qinghai–Tibet engineering corridor, China. *Remote Sensing*, *15*(15), 3728. https://doi.org/10.3390/rs15153728

Eggleston, J., & Pope, J. (2013). *Land subsidence and relative sea-level rise in the southern Chesapeake Bay region (Circular No. Circular 1392)* (p. 24). USGS.

Erkens, G., van der Meulen, M. J., & Middelkoop, H. (2016). Double trouble: Subsidence and CO_2 respiration due to 1,000 years of Dutch coastal peatlands cultivation. *Hydrogeology Journal*, *24*(3), 551–568. https://doi.org/10.1007/s10040-016-1380-4

Erten, E., Reigber, A., & Hellwich, O. (2010). Generation of three-dimensional deformation maps from InSAR data using spectral diversity techniques. *ISPRS Journal of Photogrammetry and Remote Sensing*, *65*(4), 388–394. https://doi.org/10.1016/j.isprsjprs.2010.04.005

Eshqi Molan, Y., Kim, J.-W., Lu, Z., Wylie, B., & Zhu, Z. (2018). Modeling wildfire-induced permafrost deformation in an Alaskan boreal forest using InSAR observations. *Remote Sensing*, *10*(3), 405. https://doi.org/10.3390/rs10030405

Ezquerro, P., Herrera, G., Marchamalo, M., Tomás, R., Béjar-Pizarro, M., & Martínez, R. (2014). A quasi-elastic aquifer deformational behavior: Madrid aquifer case study. *Journal of Hydrology*, *519*, 1192–1204. https://doi.org/10.1016/j.jhydrol.2014.08.040

Famiglietti, J. S. (2014). The global groundwater crisis. *Nature Climate Change*, *4*(11), 945–948. https://doi.org/10.1038/nclimate2425

Faunt, C. C., Sneed, M., Traum, J., & Brandt, J. T. (2016). Water availability and land subsidence in the Central Valley, California, USA. *Hydrogeology Journal*, *24*(3), 675–684. https://doi.org/10.1007/s10040-015-1339-x

Ferretti, A., Colombo, D., Fumagalli, A., Novali, F., & Rucci, A. (2015). InSAR data for monitoring land subsidence: Time to think big. *Proceedings of the International Association of Hydrological Sciences*, *372*, 331–334. https://doi.org/10.5194/piahs-372-331-2015

Ferretti, A., Monti-Guarnieri, A., Prati, C., & Rocca, F. (2007). *InSar Principles: Guidelines for SAR interferometry processing and interpretation (No. TM-19)* (p. 250). ESA Publications.

Ferretti, A., Prati, C., & Rocca, F. (2001). Permanent scatterers in SAR interferometry. *IEEE Transactions on Geoscience and Remote Sensing*, *39*(1), 8–20. https://doi.org/10.1109/36.898661

Fielding, E. J., Blom, R. G., & Goldstein, R. M. (1998). Rapid subsidence over oil fields measured by SAR interferometry. *Geophysical Research Letters*, *25*(17), 3215–3218. https://doi.org/10.1029/98GL52260

Forkuor, G., Conrad, C., Thiel, M., Ullmann, T., & Zoungrana, E. (2014). Integration of optical and synthetic aperture radar imagery for improving crop mapping in northwestern Benin, West Africa. *Remote Sensing*, *6*(7), 6472–6499. https://doi.org/10.3390/rs6076472

Gabrysch, R. K., & Neighbors, R. J. (2005). Measuring a century of subsidence in the Houston-Galveston region, Texas, USA. In *Proceedings of the seventh international symposium on land subsidence* (pp. 379–387).

Galloway, D. L., & Burbey, T. J. (2011). Review: Regional land subsidence accompanying groundwater extraction. *Hydrogeology Journal*, *19*(8), 1459–1486. https://doi.org/10.1007/s10040-011-0775-5

Galloway, D. L., & Hoffmann, J. (2007). The application of satellite differential SAR interferometry-derived ground displacements in hydrogeology. *Hydrogeology Journal*, *15*(1), 133–154. https://doi.org/10.1007/s10040-006-0121-5

Gambolati, G., Teatini, P., & Ferronato, M. (2005). Anthropogenic land subsidence. In M. G. Anderson, & J. J. McDonnell (Eds.), *Encyclopedia of hydrological sciences* (p. hsa164b). John Wiley & Sons, Ltd. https://doi.org/10.1002/0470848944.hsa164b

Ganju, N. K., Kirwan, M. L., Dickhudt, P. J., Guntenspergen, G. R., Cahoon, D. R., & Kroeger, K. D. (2015). Sediment transport-based metrics of wetland stability. *Geophysical Research Letters*, *42*(19), 7992–8000. https://doi.org/10.1002/2015GL065980

Garg, S., Motagh, M., Indu, J., & Karanam, V. (2022). Tracking hidden crisis in India's capital from space: Implications of unsustainable groundwater use. *Scientific Reports*, *12*(1), 651. https://doi.org/10.1038/s41598-021-04193-9

Ge, L., Li, X., Chang, H., Ng, A. H., Zhang, K., & Hu, Z. (2010). Impact of ground subsidence on the Beijing–Tianjin high-speed railway as mapped by radar interferometry. *Annals of GIS*, *16*(2), 91–102. https://doi.org/10.1080/19475683.2010.492125

Ghorbani, Z., Khosravi, A., Maghsoudi, Y., Mojtahedi, F. F., Javadnia, E., & Nazari, A. (2022). Use of InSAR data for measuring land subsidence induced by groundwater withdrawal and climate change in Ardabil Plain, Iran. *Scientific Reports*, *12*(1), 13998. https://doi.org/10.1038/s41598-022-17438-y

Gibson, C. M., Brinkman, T., Cold, H., Brown, D., & Turetsky, M. (2021). Identifying increasing risks of hazards for northern land-users caused by permafrost thaw: Integrating scientific and community-based research approaches. *Environmental Research Letters*, *16*(6), 064047. https://doi.org/10.1088/1748-9326/abfc79

Gibson, C. M., Chasmer, L. E., Thompson, D. K., Quinton, W. L., Flannigan, M. D., & Olefeldt, D. (2018). Wildfire as a major driver of recent permafrost thaw in boreal peatlands. *Nature Communications*, *9*(1), 3041. https://doi.org/10.1038/s41467-018-05457-1

Giosan, L., Syvitski, J., Constantinescu, S., & Day, J. (2014). Climate change: Protect the world's deltas. *Nature*, *516*(7529), 31–33. https://doi.org/10.1038/516031a

Gong, H., Pan, Y., Zheng, L., Li, X., Zhu, L., Zhang, C., et al. (2018). Long-term groundwater storage changes and land subsidence development in the North China Plain (1971–2015). *Hydrogeology Journal*, *26*(5), 1417–1427. https://doi.org/10.1007/s10040-018-1768-4

Grall, C., Steckler, M. S., Pickering, J. L., Goodbred, S., Sincavage, R., Paola, C., et al. (2018). A base-level stratigraphic approach to determining Holocene subsidence of the Ganges–Meghna–Brahmaputra Delta plain. *Earth and Planetary Science Letters*, *499*, 23–36. https://doi.org/10.1016/j.epsl.2018.07.008

Greve, P., Orlowsky, B., Mueller, B., Sheffield, J., Reichstein, M., & Seneviratne, S. I. (2014). Global assessment of trends in wetting and drying over land. *Nature Geoscience*, *7*(10), 716–721. https://doi.org/10.1038/ngeo2247

Gurevich, A. E., & Chilingarian, G. V. (1993). Subsidence over producing oil and gas fields, and gas leakage to the surface. *Journal of Petroleum Engineering and Science*, *9*(3), 239–250. https://doi.org/10.1016/0920-4105(93)90017-9

Hachez-Leroy, F. (2014). *Industrial Heritage in the Nord–Pas-de-Calais/Le patrimoine industriel du Nord–Pas-de-Calais* (pp. 6–25). Patrimoine Industriel (Former L'Archéologie Industrielle).

Haghshenas Haghighi, M., & Motagh, M. (2019). Ground surface response to continuous compaction of aquifer system in Tehran, Iran: Results from a long-term multi-sensor InSAR analysis. *Remote Sensing of Environment*, *221*, 534–550. https://doi.org/10.1016/j.rse.2018.11.003

Hallegatte, S., Green, C., Nicholls, R. J., & Corfee-Morlot, J. (2013). Future flood losses in major coastal cities. *Nature Climate Change*, *3*(9), 802–806. https://doi.org/10.1038/nclimate1979

Hao, Z., Singh, V. P., & Xia, Y. (2018). Seasonal drought prediction: Advances, challenges, and future prospects. *Reviews of Geophysics*, *56*(1), 108–141. https://doi.org/10.1002/2016RG000549

Hassani, A., Azapagic, A., & Shokri, N. (2021). Global predictions of primary soil salinization under changing climate in the 21st century. *Nature Communications*, *12*(1), 6663. https://doi.org/10.1038/s41467-021-26907-3

Hayashi, T., Tokunaga, T., Aichi, M., Shimada, J., & Taniguchi, M. (2009). Effects of human activities and urbanization on groundwater environments: An example from the aquifer system of Tokyo and the surrounding area. *Science of the Total Environment*, *407*(9), 3165–3172. https://doi.org/10.1016/j.scitotenv.2008.07.012

Herrera-García, G., Ezquerro, P., Tomás, R., Béjar-Pizarro, M., López-Vinielles, J., Rossi, M., et al. (2021). Mapping the global threat of land subsidence. *Science*, *371*(6524), 34–36. https://doi.org/10.1126/science.abb8549

Hjort, J., Streletskiy, D., Doré, G., Wu, Q., Bjella, K., & Luoto, M. (2022). Impacts of permafrost degradation on infrastructure. *Nature Reviews Earth & Environment*, *3*(1), 24–38. https://doi.org/10.1038/s43017-021-00247-8

Hoekstra, A. Y., & Mekonnen, M. M. (2012). The water footprint of humanity. *Proceedings of the National Academy of Sciences of the United States of America*, *109*(9), 3232–3237. https://doi.org/10.1073/pnas.1109936109

Holloway, J. E., Lewkowicz, A. G., Douglas, T. A., Li, X., Turetsky, M. R., Baltzer, J. L., & Jin, H. (2020). Impact of wildfire on permafrost landscapes: A review of recent advances and future prospects. *Permafrost and Periglacial Processes*, *31*(3), 371–382. https://doi.org/10.1002/ppp.2048

Holtz, R. D., & Kovacs, W. D. (1981). *An introduction to geotechnical engineering*. Prentice Hall.

Holzer, T. L., & Bluntzer, R. L. (1984). Land subsidence near oil and gas fields, Houston, Texas. *Groundwater*, *22*(4), 450–459. https://doi.org/10.1111/j.1745-6584.1984.tb01416.x

Hooijer, A., Page, S., Jauhiainen, J., Lee, W. A., Lu, X. X., Idris, A., & Anshari, G. (2012). Subsidence and carbon loss in drained tropical peatlands. *Biogeosciences*, *9*(3), 1053–1071. https://doi.org/10.5194/bg-9-1053-2012

Hoyt, A. M., Chaussard, E., Seppalainen, S. S., & Harvey, C. F. (2020). Widespread subsidence and carbon emissions across southeast Asian peatlands. *Nature Geoscience*, *13*(6), 435–440. https://doi.org/10.1038/s41561-020-0575-4

Hu, B., Wang, H.-S., Sun, Y.-L., Hou, J.-G., & Liang, J. (2014). Long-term land subsidence monitoring of Beijing (China) using the small baseline subset (SBAS) technique. *Remote Sensing*, *6*(5), 3648–3661. https://doi.org/10.3390/rs6053648

Hu, R. L., Yue, Z. Q., Wang, L. C., & Wang, S. J. (2004). Review on current status and challenging issues of land subsidence in China. *Engineering Geology*, *76*(1–2), 65–77. https://doi.org/10.1016/j.enggeo.2004.06.006

Hugelius, G., Loisel, J., Chadburn, S., Jackson, R. B., Jones, M., MacDonald, G., et al. (2020). Large stocks of peatland carbon and nitrogen are vulnerable to permafrost thaw. *Proceedings of the National Academy of Sciences of the United States of America*, *117*(34), 20438–20446. https://doi.org/10.1073/pnas.1916387117

Huning, L. S., & AghaKouchak, A. (2018). Mountain snowpack response to different levels of warming. *Proceedings of the National Academy of Sciences of the United States of America*, *115*(43), 10932–10937. https://doi.org/10.1073/pnas.1805953115

Huning, L. S., & AghaKouchak, A. (2020). Global snow drought hot spots and characteristics. *Proceedings of the National Academy of Sciences of the United States of America*, *117*(33), 19753–19759. https://doi.org/10.1073/pnas.1915921117

IPCC. (2019). In P. R. Shukla, J. Skea, E. C. Buendia, V. Masson-Delmotte, H. O. Pörtner, et al. (Eds.), *Climate change and land: An IPCC special report on climate change, desertification, land degradation, sustainable land management, food security, and greenhouse gas fluxes in terrestrial ecosystems*. (In press).

IPCC. (2021). In V. Masson-Delmotte, P. Zhai, A. Pirani, S. L. Conners, C. Péan, et al. (Eds.), *Climate change 2021: The physical science basis. Contribution of working group I to the sixth assessment report of the Intergovernmental Panel on Climate Change*. Cambridge University Press. (In Press).

Jago-on, K. A. B., Kaneko, S., Fujikura, R., Fujiwara, A., Imai, T., Matsumoto, T., et al. (2009). Urbanization and subsurface environmental issues: An attempt at DPSIR model application in Asian cities. *Science of the Total Environment*, *407*(9), 3089–3104. https://doi.org/10.1016/j.scitotenv.2008.08.004

Jeanne, P., Farr, T. G., Rutqvist, J., & Vasco, D. W. (2019). Role of agricultural activity on land subsidence in the San Joaquin Valley, California. *Journal of Hydrology*, *569*, 462–469. https://doi.org/10.1016/j.jhydrol.2018.11.077

Kaat, A., & Joosten, H. (2009). *Fact book for UNFCCC policies on peat carbon emissions* (p. 24). Wetlands International. Retrieved from https://www.wetlands.org/publications/fact-book-for-unfccc-policies-on-peat-carbon-emissions/

Karjalainen, O., Luoto, M., Aalto, J., Etzelmüller, B., Grosse, G., Jones, B. M., et al. (2020). High potential for loss of permafrost landforms in a changing climate. *Environmental Research Letters*, *15*(10), 104065. https://doi.org/10.1088/1748-9326/abafd5

Kasischke, E. S., Bourgeau-Chavez, L. L., & Johnstone, J. F. (2007). Assessing spatial and temporal variations in surface soil moisture in fire-disturbed black spruce forests in Interior Alaska using spaceborne synthetic aperture radar imagery—Implications for post-fire tree recruitment. *Remote Sensing of Environment*, *108*(1), 42–58. https://doi.org/10.1016/j.rse.2006.10.020

Khorrami, M., Shirzaei, M., Ghobadi-Far, K., Werth, S., Carlson, G., & Zhai, G. (2023). Groundwater volume loss in Mexico City constrained by InSAR and GRACE observations and mechanical models. *Geophysical Research Letters*, *50*(5), e2022GL101962. https://doi.org/10.1029/2022GL101962

Kirwan, M. L., & Gedan, K. B. (2019). Sea-level driven land conversion and the formation of ghost forests. *Nature Climate Change*, *9*(6), 450–457. https://doi.org/10.1038/s41558-019-0488-7

Klein, E., Vigny, C., Fleitout, L., Grandin, R., Jolivet, R., Rivera, E., & Métois, M. (2017). A comprehensive analysis of the Illapel 2015 Mw8.3 earthquake from GPS and InSAR data. *Earth and Planetary Science Letters*, *469*, 123–134. https://doi.org/10.1016/j.epsl.2017.04.010

Knutson, T. R., McBride, J. L., Chan, J., Emanuel, K., Holland, G., Landsea, C., et al. (2010). Tropical cyclones and climate change. *Nature Geoscience*, *3*(3), 157–163. https://doi.org/10.1038/ngeo779

Kondolf, G. M., Schmitt, R. J. P., Carling, P. A., Goichot, M., Keskinen, M., Arias, M. E., et al. (2022). Save the Mekong Delta from drowning. *Science*, *376*(6593), 583–585. https://doi.org/10.1126/science.abm5176

Langenbrunner, B., Neelin, J. D., Lintner, B. R., & Anderson, B. T. (2015). Patterns of precipitation change and climatological uncertainty among CMIP5 models, with a focus on the midlatitude Pacific storm track. *Journal of Climate*, *28*(19), 7857–7872. https://doi.org/10.1175/JCLI-D-14-00800.1

Levy, M. C., Neely, W. R., Borsa, A. A., & Burney, J. A. (2020). Fine-scale spatiotemporal variation in subsidence across California's San Joaquin Valley explained by groundwater demand. *Environmental Research Letters*, *15*(10), 104083. https://doi.org/10.1088/1748-9326/abb55c

Li, M.-G., Chen, J.-J., Xu, Y.-S., Tong, D.-G., Cao, W.-W., & Shi, Y.-J. (2021). Effects of groundwater exploitation and recharge on land subsidence and infrastructure settlement patterns in Shanghai. *Engineering Geology*, *282*, 105995. https://doi.org/10.1016/j.enggeo.2021.105995

Liu, Y., Li, J., Fasullo, J., & Galloway, D. L. (2020). Land subsidence contributions to relative sea level rise at tide gauge Galveston Pier 21, Texas. *Scientific Reports*, *10*(1), 17905. https://doi.org/10.1038/s41598-020-74696-4

Liu, Z., Fagherazzi, S., & Cui, B. (2021). Success of coastal wetlands restoration is driven by sediment availability. *Communications Earth & Environment*, *2*(1), 44. https://doi.org/10.1038/s43247-021-00117-7

Mahmoudpour, M., Khamehchiyan, M., Nikudel, M. R., & Ghassemi, M. R. (2013). Characterization of regional land subsidence induced by groundwater withdrawals in Tehran, Iran. *Geopersia*, *3*(2), 49–62. https://doi.org/10.22059/JGEOPE.2013.36014

Marino, G. G., & Gamble, W. (1986). Mine subsidence damage from room and pillar mining in Illinois. *International Journal of Mining and Geological Engineering*, *4*(2), 129–150. https://doi.org/10.1007/bf01560671

Marker, B. R. (2013). Land subsidence. In P. T. Bobrowsky (Ed.), *Encyclopedia of natural hazards* (pp. 583–590). Springer.

Mazdiyasni, O., & AghaKouchak, A. (2015). Substantial increase in concurrent droughts and heatwaves in the United States. *Proceedings of the National Academy of Sciences of the United States of America*, *112*(37), 11484–11489. https://doi.org/10.1073/pnas.1422945112

Meldebekova, G., Yu, C., Li, Z., & Song, C. (2020). Quantifying ground subsidence associated with aquifer overexploitation using space-borne radar interferometry in Kabul, Afghanistan. *Remote Sensing*, *12*(15), 2461. https://doi.org/10.3390/rs12152461

Melvin, A. M., Larsen, P., Boehlert, B., Neumann, J. E., Chinowsky, P., Espinet, X., et al. (2017). Climate change damages to Alaska public infrastructure and the economics of proactive adaptation. *Proceedings of the National Academy of Sciences of the United States of America*, *114*(2). https://doi.org/10.1073/pnas.1611056113

Merryman Boncori, J. P. (2019). Measuring coseismic deformation with spaceborne synthetic aperture radar: A review. *Frontiers in Earth Science*, *7*, 16. https://doi.org/10.3389/feart.2019.00016

Miller, M. M., Jones, C. E., Sangha, S. S., & Bekaert, D. P. (2020). Rapid drought-induced land subsidence and its impact on the California aqueduct. *Remote Sensing of Environment*, *251*, 112063. https://doi.org/10.1016/j.rse.2020.112063

Miller, M. M., & Shirzaei, M. (2015). Spatiotemporal characterization of land subsidence and uplift in Phoenix using InSAR time series and wavelet transforms. *Journal of Geophysical Research: Solid Earth*, *120*(8), 5822–5842. https://doi.org/10.1002/2015JB012017

Miller, M. M., & Shirzaei, M. (2019). Land subsidence in Houston correlated with flooding from Hurricane Harvey. *Remote Sensing of Environment*, *225*, 368–378. https://doi.org/10.1016/j.rse.2019.03.022

Miller, M. M., Shirzaei, M., & Argus, D. (2017). Aquifer mechanical properties and decelerated compaction in Tucson, Arizona. *Journal of Geophysical Research: Solid Earth*, *122*(10), 8402–8416. https://doi.org/10.1002/2017JB014531

Mishra, A. K., & Singh, V. P. (2010). A review of drought concepts. *Journal of Hydrology*, *391*(1–2), 202–216. https://doi.org/10.1016/j.jhydrol.2010.07.012

Moftakhari, H. R., AghaKouchak, A., Sanders, B. F., Allaire, M., & Matthew, R. A. (2018). What is nuisance flooding? Defining and monitoring an emerging challenge. *Water Resources Research*, *54*(7), 4218–4227. https://doi.org/10.1029/2018WR022828

Motagh, M., Shamshiri, R., Haghshenas Haghighi, M., Wetzel, H.-U., Akbari, B., Nahavandchi, H., et al. (2017). Quantifying groundwater exploitation induced subsidence in the Rafsanjan plain, southeastern Iran, using InSAR time-series and in situ measurements. *Engineering Geology*, *218*, 134–151. https://doi.org/10.1016/j.enggeo.2017.01.011

Motagh, M., Walter, T. R., Sharifi, M. A., Fielding, E., Schenk, A., Anderssohn, J., & Zschau, J. (2008). Land subsidence in Iran caused by widespread water reservoir overexploitation. *Geophysical Research Letters*, *35*(16), L16403. https://doi.org/10.1029/2008GL033814

Mount, J., & Twiss, R. (2005). Subsidence, sea level rise, and seismicity in the Sacramento–San Joaquin Delta. *San Francisco Estuary and Watershed Science*, *3*(1). https://doi.org/10.15447/sfews.2005v3iss1art7

Musa, Z. N., Popescu, I., & Mynett, A. (2015). A review of applications of satellite SAR, optical, altimetry and DEM data for surface water modelling, mapping and parameter estimation. *Hydrology and Earth System Sciences*, *19*(9), 3755–3769. https://doi.org/10.5194/hess-19-3755-2015

Nawaz, M. F., Bourrié, G., & Trolard, F. (2013). Soil compaction impact and modelling. A review. *Agronomy for Sustainable Development*, *33*(2), 291–309. https://doi.org/10.1007/s13593-011-0071-8

Neely, W. R., Borsa, A. A., Burney, J. A., Levy, M. C., Silverii, F., & Sneed, M. (2021). Characterization of groundwater recharge and flow in California's San Joaquin Valley from InSAR-observed surface deformation. *Water Resources Research*, *57*(4), e2020WR028451. https://doi.org/10.1029/2020WR028451

Ng, A. H.-M., Ge, L., & Li, X. (2015). Assessments of land subsidence in the Gippsland Basin of Australia using ALOS PALSAR data. *Remote Sensing of Environment*, *159*, 86–101. https://doi.org/10.1016/j.rse.2014.12.003

Nicholls, R. J., Lincke, D., Hinkel, J., Brown, S., Vafeidis, A. T., Meyssignac, B., et al. (2021). A global analysis of subsidence, relative sea-level change and coastal flood exposure. *Nature Climate Change*, *11*(4), 338–342. https://doi.org/10.1038/s41558-021-00993-z

Nicholls, R. J., & Shirzaei, M. (2024). Earth's sinking surface. *Science*, *384*(6693), 268–269. https://doi.org/10.1126/science.ado9986

Nitzbon, J., Westermann, S., Langer, M., Martin, L. C. P., Strauss, J., Laboor, S., & Boike, J. (2020). Fast response of cold ice-rich permafrost in northeast Siberia to a warming climate. *Nature Communications*, *11*(1), 2201. https://doi.org/10.1038/s41467-020-15725-8

NOAA. (2018). *August/September 2017 Hurricane Harvey* (p. 58). Silver Spring. Retrieved from https://www.weather.gov/media/publications/assessments/harvey6-18.pdf

Ohenhen, L. O., Shirzaei, M., & Barnard, P. L. (2024). Slowly but surely: Exposure of communities and infrastructure to subsidence on the US east coast. *PNAS Nexus*, *3*(1), pgad426. https://doi.org/10.1093/pnasnexus/pgad426

Ohenhen, L. O., Shirzaei, M., Ojha, C., & Kirwan, M. L. (2023). Hidden vulnerability of US Atlantic coast to sea-level rise due to vertical land motion. *Nature Communications*, *14*(1), 2038. https://doi.org/10.1038/s41467-023-37853-7

Ohenhen, L. O., Shirzaei, M., Ojha, C., Sherpa, S. F., & Nicholls, R. J. (2024). Disappearing cities on US coasts. *Nature*, *627*(8002), 108–115. https://doi.org/10.1038/s41586-024-07038-3

Ojha, C., Werth, S., & Shirzaei, M. (2020). Recovery of aquifer-systems in southwest US following 2012–2015 drought: Evidence from InSAR, GRACE and groundwater level data. *Journal of Hydrology*, *587*, 124943. https://doi.org/10.1016/j.jhydrol.2020.124943

Oppenheimer, M., Glavovic, B. C., Hinkel, J., van de Wal, R., Magnan, A. K., Abd-Elgawad, A., et al. (2019). Sea level rise and implications for low-lying islands, coasts and communities. In *IPCC special report on the ocean and cryosphere in a changing climate* (pp. 321–445). In press.

Ottinger, M., & Kuenzer, C. (2020). Spaceborne L-band synthetic aperture radar data for geoscientific analyses in coastal land applications: A review. *Remote Sensing*, *12*(14), 2228. https://doi.org/10.3390/rs12142228

Ouchi, K. (2013). Recent trend and advance of synthetic aperture radar with selected topics. *Remote Sensing*, *5*(2), 716–807. https://doi.org/10.3390/rs5020716

Padrón, R. S., Gudmundsson, L., Decharme, B., Ducharne, A., Lawrence, D. M., Mao, J., et al. (2020). Observed changes in dry-season water availability attributed to human-induced climate change. *Nature Geoscience*, *13*(7), 477–481. https://doi.org/10.1038/s41561-020-0594-1

Parsons, T., Wu, P., Wei, M., & D'Hondt, S. (2023). The weight of New York City: Possible contributions to subsidence from anthropogenic sources. *Earth's Future*, *11*(5), e2022EF003465. https://doi.org/10.1029/2022EF003465

Peltier, A., Bianchi, M., Kaminski, E., Komorowski, J.-C., Rucci, A., & Staudacher, T. (2010). PSInSAR as a new tool to monitor pre-eruptive volcano ground deformation: Validation using GPS measurements on Piton de la Fournaise. *Geophysical Research Letters*, *37*(12), L12301. https://doi.org/10.1029/2010GL043846

Peng, S. S. (2008). Coal mine ground control (No. OSTI 21149595).

Pronger, J., Schipper, L. A., Hill, R. B., Campbell, D. I., & McLeod, M. (2014). Subsidence rates of drained agricultural peatlands in New Zealand and the relationship with time since drainage. *Journal of Environmental Quality*, *43*(4), 1442–1449. https://doi.org/10.2134/jeq2013.12.0505

Qin, Y., Abatzoglou, J. T., Siebert, S., Huning, L. S., AghaKouchak, A., Mankin, J. S., et al. (2020). Agricultural risks from changing snowmelt. *Nature Climate Change*, *10*(5), 459–465. https://doi.org/10.1038/s41558-020-0746-8

Qiu, C., Ciais, P., Zhu, D., Guenet, B., Peng, S., Petrescu, A. M. R., et al. (2021). Large historical carbon emissions from cultivated northern peatlands. *Science Advances*, *7*(23), eabf1332. https://doi.org/10.1126/sciadv.abf1332

Qu, F., Lu, Z., Kim, J., & Turco, M. J. (2023). Mapping and characterizing land deformation during 2007–2011 over the Gulf Coast by L-band InSAR. *Remote Sensing of Environment*, *284*, 113342. https://doi.org/10.1016/j.rse.2022.113342

Ramage, J., Jungsberg, L., Wang, S., Westermann, S., Lantuit, H., & Heleniak, T. (2021). Population living on permafrost in the Arctic. *Population and Environment*, *43*(1), 22–38. https://doi.org/10.1007/s11111-020-00370-6

Raspini, F., Caleca, F., Del Soldato, M., Festa, D., Confuorto, P., & Bianchini, S. (2022). Review of satellite radar interferometry for subsidence analysis. *Earth-Science Reviews*, *235*, 104239. https://doi.org/10.1016/j.earscirev.2022.104239

Raucoules, D., Colesanti, C., & Carnec, C. (2007). Use of SAR interferometry for detecting and assessing ground subsidence. *Comptes Rendus Geoscience*, *339*(5), 289–302. https://doi.org/10.1016/j.crte.2007.02.002

Richey, A. S., Thomas, B. F., Lo, M., Reager, J. T., Famiglietti, J. S., Voss, K., et al. (2015). Quantifying renewable groundwater stress with GRACE. *Water Resources Research*, *51*(7), 5217–5238. https://doi.org/10.1002/2015WR017349

Robinson, J. D., & Vahedifard, F. (2016). Weakening mechanisms imposed on California's levees under multiyear extreme drought. *Climatic Change*, *137*(1–2), 1–14. https://doi.org/10.1007/s10584-016-1649-6

Rodell, M., Famiglietti, J. S., Wiese, D. N., Reager, J. T., Beaudoing, H. K., Landerer, F. W., & Lo, M.-H. (2018). Emerging trends in global freshwater availability. *Nature*, *557*(7707), 651–659. https://doi.org/10.1038/s41586-018-0123-1

Rosen, P. A., Hensley, S., Joughin, I. R., Li, F. K., Madsen, S. N., Rodríguez, E., & Goldstein, R. M. (2000). Synthetic aperture radar interferometry. *Proceedings of the IEEE*, *88*(3), 50–382. https://doi.org/10.1109/5.838084

Samsonov, S. V., d'Oreye, N., & Smets, B. (2013). Ground deformation associated with post-mining activity at the French–German border revealed by novel InSAR time series method. *International Journal of Applied Earth Observation and Geoinformation*, *23*, 142–154. https://doi.org/10.1016/j.jag.2012.12.008

Sánchez-Gámez, P., & Navarro, F. (2017). Glacier surface velocity retrieval using D-InSAR and offset tracking techniques applied to ascending and descending passes of Sentinel-1 data for southern Ellesmere ice caps, Canadian Arctic. *Remote Sensing*, *9*(5), 442. https://doi.org/10.3390/rs9050442

Shen, M., Chen, J., Zhuan, M., Chen, H., Xu, C.-Y., & Xiong, L. (2018). Estimating uncertainty and its temporal variation related to global climate models in quantifying climate change impacts on hydrology. *Journal of Hydrology*, *556*, 10–24. https://doi.org/10.1016/j.jhydrol.2017.11.004

Sherpa, S. F., Shirzaei, M., & Ojha, C. (2023). Disruptive role of vertical land motion in future assessments of climate change-driven sea-level rise and coastal flooding hazards in the Chesapeake Bay. *Journal of Geophysical Research: Solid Earth*, *128*(4), e2022JB025993. https://doi.org/10.1029/2022JB025993

Shi, Y.-J., Li, M.-G., Chen, J.-J., & Wang, J.-H. (2018). Long-term settlement behavior of a highway in land subsidence area. *Journal of Performance of Constructed Facilities*, *32*(5), 04018063. https://doi.org/10.1061/(ASCE)CF.1943-5509.0001195

Shiklomanov, N. I., Streletskiy, D. A., Grebenets, V. I., & Suter, L. (2017). Conquering the permafrost: Urban infrastructure development in Norilsk, Russia. *Polar Geography*, *40*(4), 273–290. https://doi.org/10.1080/1088937X.2017.1329237

Shirzaei, M., & Bürgmann, R. (2018). Global climate change and local land subsidence exacerbate inundation risk to the San Francisco Bay area. *Science Advances*, *4*(3), eaap9234. https://doi.org/10.1126/sciadv.aap9234

Shirzaei, M., Freymueller, J., Törnqvist, T. E., Galloway, D. L., Dura, T., & Minderhoud, P. S. J. (2021). Measuring, modelling and projecting coastal land subsidence. *Nature Reviews Earth & Environment*, *2*(1), 40–58. https://doi.org/10.1038/s43017-020-00115-x

Showstack, R. (2014). Scientists focus on land subsidence impacts on coastal and delta cities. *Eos, Transactions American Geophysical Union*, *95*(19), 159. https://doi.org/10.1002/2014EO190003

Siebert, S., Kummu, M., Porkka, M., Döll, P., Ramankutty, N., & Scanlon, B. (2015). A global data set of the extent of irrigated land from 1900 to 2005. *Hydrology and Earth System Sciences*, *19*(3), 1521–1545. https://doi.org/10.5194/hess-19-1521-2015

Siirila-Woodburn, E., Rhoades, A. M., Hatchett, B. J., Huning, L. S., Szinai, J., Tague, C., et al. (2021). A low-to-no snow future and its impacts on water resources in the western United States. *Nature Reviews Earth & Environment*, *2*(11), 800–819. https://doi.org/10.1038/s43017-021-00219-y

Siriwardane-de Zoysa, R., Schöne, T., Herbeck, J., Illigner, J., Haghighi, M., Simarmata, H., et al. (2021). The 'wickedness' of governing land subsidence: Policy perspectives from urban Southeast Asia. *PLoS One*, *16*(6), e0250208. https://doi.org/10.1371/journal.pone.0250208

Smart, L. S., Taillie, P. J., Poulter, B., Vukomanovic, J., Singh, K. K., Swenson, J. J., et al. (2020). Aboveground carbon loss associated with the spread of ghost forests as sea levels rise. *Environmental Research Letters*, *15*(10), 104028. https://doi.org/10.1088/1748-9326/aba136

Smith, R., & Knight, R. (2019). Modeling land subsidence using InSAR and airborne electromagnetic data. *Water Resources Research*, *55*(4), 2801–2819. https://doi.org/10.1029/2018WR024185
Sophocleous, M. (2005). Groundwater recharge and sustainability in the High Plains aquifer in Kansas, USA. *Hydrogeology Journal*, *13*(2), 351–365. https://doi.org/10.1007/s10040-004-0385-6
Sousa, J. J., Ruiz, A. M., Hanssen, R. F., Bastos, L., Gil, A. J., Galindo-Zaldívar, J., & Sanz de Galdeano, C. (2010). PS-InSAR processing methodologies in the detection of field surface deformation—Study of the Granada basin (Central Betic Cordilleras, southern Spain). *Journal of Geodynamics*, *49*(3–4), 181–189. https://doi.org/10.1016/j.jog.2009.12.002
Stancliff, R. P. W., & van der Kooij, M. W. A. (2001). The use of satellite-based radar interferometry to monitor production activity at the Cold Lake heavy oil field, Alberta, Canada. *AAPG Bulletin*, *85*. https://doi.org/10.1306/8626C9FB-173B-11D7-8645000102C1865D
Stephens, J. C., Allen, L. H., & Chen, E. (1984). Organic soil subsidence. In T. L. Holzer (Ed.), *Man-induced land subsidence* (Vol. VI, pp. 107–122). Geological Society of America. https://doi.org/10.1130/reg6-p107
Streletskiy, D., Anisimov, O., & Vasiliev, A. (2015). Permafrost degradation. In *Snow and ice-related hazards, risks, and disasters* (pp. 303–344). Elsevier. https://doi.org/10.1016/B978-0-12-394849-6.00010-X
Svoboda, M., & Fuchs, B. A. (2016). *Handbook of drought indicators and indices*. World Meteorological Organization. Retrieved from http://www.droughtmanagement.info/handbook-drought-indicators-and-indices/
Sweet, W., Park, J., Marra, J., Zervas, C., & Gill, S. (2014). Sea level rise and nuisance flood frequency changes around the United States. NOAA Technical Report NOS CO-OPS 073. https://repository.library.noaa.gov/view/noaa/30823
Syvitski, J. P. M., Kettner, A. J., Overeem, I., Hutton, E. W. H., Hannon, M. T., Brakenridge, G. R., et al. (2009). Sinking deltas due to human activities. *Nature Geoscience*, *2*(10), 681–686. https://doi.org/10.1038/ngeo629
Tang, W., Zhao, X., Motagh, M., Bi, G., Li, J., Chen, M., et al. (2022). Land subsidence and rebound in the Taiyuan basin, northern China, in the context of inter-basin water transfer and groundwater management. *Remote Sensing of Environment*, *269*, 112792. https://doi.org/10.1016/j.rse.2021.112792
Teatini, P., Ferronato, M., Gambolati, G., Bertoni, W., & Gonella, M. (2005). A century of land subsidence in Ravenna, Italy. *Environmental Geology*, *47*(6), 831–846. https://doi.org/10.1007/s00254-004-1215-9
Tessler, Z. D., Vörösmarty, C. J., Grossberg, M., Gladkova, I., Aizenman, H., Syvitski, J. P. M., & Foufoula-Georgiou, E. (2015). Profiling risk and sustainability in coastal deltas of the world. *Science*, *349*(6248), 638–643. https://doi.org/10.1126/science.aab3574
Tilman, D., Balzer, C., Hill, J., & Befort, B. L. (2011). Global food demand and the sustainable intensification of agriculture. *Proceedings of the National Academy of Sciences of the United States of America*, *108*(50), 20260–20264. https://doi.org/10.1073/pnas.1116437108
Tiwari, D. K., Hari, M., Kundu, B., Jha, B., Tyagi, B., & Malik, K. (2023). Delhi urbanization footprint and its effect on the Earth's subsurface state-of-stress through decadal seismicity modulation. *Scientific Reports*, *13*(1), 11750. https://doi.org/10.1038/s41598-023-38348-7
Tsokas, A., Rysz, M., Pardalos, P. M., & Dipple, K. (2022). SAR data applications in Earth observation: An overview. *Expert Systems with Applications*, *205*, 117342. https://doi.org/10.1016/j.eswa.2022.117342
Tsyganskaya, V., Martinis, S., Marzahn, P., & Ludwig, R. (2018). SAR-based detection of flooded vegetation—A review of characteristics and approaches. *International Journal of Remote Sensing*, *39*(8), 2255–2293. https://doi.org/10.1080/01431161.2017.1420938
Turetsky, M. R., Abbott, B. W., Jones, M. C., Anthony, K. W., Olefeldt, D., Schuur, E. A. G., et al. (2020). Carbon release through abrupt permafrost thaw. *Nature Geoscience*, *13*(2), 138–143. https://doi.org/10.1038/s41561-019-0526-0
Tzampoglou, P., & Loupasakis, C. (2018). Evaluating geological and geotechnical data for the study of land subsidence phenomena at the perimeter of the Amyntaio coalmine, Greece. *International Journal of Mining Science and Technology*, *28*(4), 601–612. https://doi.org/10.1016/j.ijmst.2017.11.002
Ullah, A., Bano, A., & Khan, N. (2021). Climate change and salinity effects on crops and chemical communication between plants and plant growth-promoting microorganisms under stress. *Frontiers in Sustainable Food Systems*, *5*, 618092. https://doi.org/10.3389/fsufs.2021.618092
UNESCO. (n.d.). UNESCO land subsidence international initiative. Retrieved from https://www.landsubsidence-unesco.org/
Vahedifard, F., Abdollahi, M., Leshchinsky, B. A., Stark, T. D., Sadegh, M., & AghaKouchak, A. (2024). Interdependencies between wildfire-induced alterations in soil properties, near-surface processes, and geohazards. *Earth and Space Science*, *11*(2), e2023EA003498. https://doi.org/10.1029/2023EA003498
Vahedifard, F., Goodman, C. C., Paul, V., & AghaKouchak, A. (2024). Amplifying feedback loop between drought, soil desiccation cracking, and greenhouse gas emissions. *Environmental Research Letters*, *19*(3), 031005. https://doi.org/10.1088/1748-9326/ad2c23
Vahedifard, F., Robinson, J. D., & AghaKouchak, A. (2016). Can protracted drought undermine the structural integrity of California's earthen levees? *Journal of Geotechnical and Geoenvironmental Engineering*, *142*(6), 02516001. https://doi.org/10.1061/(ASCE)GT.1943-5606.0001465
Vitousek, S., Barnard, P. L., Fletcher, C. H., Frazer, N., Erikson, L., & Storlazzi, C. D. (2017). Doubling of coastal flooding frequency within decades due to sea-level rise. *Scientific Reports*, *7*(1), 1399. https://doi.org/10.1038/s41598-017-01362-7
Wada, Y., & Bierkens, M. F. P. (2014). Sustainability of global water use: Past reconstruction and future projections. *Environmental Research Letters*, *9*(10), 104003. https://doi.org/10.1088/1748-9326/9/10/104003
Wada, Y., van Beek, L. P. H., & Bierkens, M. F. P. (2011). Modelling global water stress of the recent past: On the relative importance of trends in water demand and climate variability. *Hydrology and Earth System Sciences*, *15*(12), 3785–3808. https://doi.org/10.5194/hess-15-3785-2011
Wahl, T., Jain, S., Bender, J., Meyers, S. D., & Luther, M. E. (2015). Increasing risk of compound flooding from storm surge and rainfall for major US cities. *Nature Climate Change*, *5*(12), 1093–1097. https://doi.org/10.1038/nclimate2736
Wang, G., & Soler, T. (2015). Measuring land subsidence using GPS: Ellipsoid height versus orthometric height. *Journal of Surveying Engineering*, *141*(2), 05014004. https://doi.org/10.1061/(ASCE)SU.1943-5428.0000137
Ward, P. J., de Ruiter, M. C., Mård, J., Schröter, K., Van Loon, A., Veldkamp, T., et al. (2020). The need to integrate flood and drought disaster risk reduction strategies. *Water Security*, *11*, 100070. https://doi.org/10.1016/j.wasec.2020.100070
Witze, A. (2020). Why Arctic fires are bad news for climate change. *Nature*, *585*(7825), 336–337. https://doi.org/10.1038/d41586-020-02568-y
Wolstencroft, M., Shen, Z., Tornqvist, T. E., Milne, G. A., & Kulp, M. (2014). Understanding subsidence in the Mississippi Delta region due to sediment, ice, and ocean loading: Insights from geophysical modeling. *Journal of Geophysical Research: Solid Earth*, *119*(4), 3838–3856. https://doi.org/10.1002/2013JB010928
Wu, P., Wei, M., & D'Hondt, S. (2022). Subsidence in coastal cities throughout the world observed by InSAR. *Geophysical Research Letters*, *49*(7), e2022GL098477. https://doi.org/10.1029/2022GL098477
Yanagiya, K., & Furuya, M. (2020). Post-wildfire surface deformation near Batagay, eastern Siberia, detected by L-Band and C-Band InSAR. *Journal of Geophysical Research: Earth Surface*, *125*(7), e2019JF005473. https://doi.org/10.1029/2019JF005473
Yin, J., Yu, D., & Wilby, R. (2016). Modelling the impact of land subsidence on urban pluvial flooding: A case study of downtown Shanghai, China. *Science of the Total Environment*, *544*, 744–753. https://doi.org/10.1016/j.scitotenv.2015.11.159

Zhang, M., & Burbey, T. J. (2016). Inverse modelling using PS-InSAR data for improved land subsidence simulation in Las Vegas Valley, Nevada: Inverse modelling using PS-InSAR data for land subsidence simulation. *Hydrological Processes*, *30*(24), 4494–4516. https://doi.org/10.1002/hyp.10945

Zhou, X., Chang, N.-B., & Li, S. (2009). Applications of SAR interferometry in Earth and environmental science research. *Sensors*, *9*(3), 1876–1912. https://doi.org/10.3390/s90301876

Zhu, L., Gong, H., Li, X., Wang, R., Chen, B., Dai, Z., & Teatini, P. (2015). Land subsidence due to groundwater withdrawal in the northern Beijing plain, China. *Engineering Geology*, *193*, 243–255. https://doi.org/10.1016/j.enggeo.2015.04.020